

FiniteFlow: multivariate functional reconstruction using finite fields and dataflow graphs

Tiziano Peraro

Physik-Institut, Universität Zürich, Wintherturerstrasse 190, CH-8057 Zürich, Switzerland

Abstract

Complex algebraic calculations can be performed by reconstructing analytic results from numerical evaluations over finite fields. We describe FINITEFLOW, a framework for defining and executing numerical algorithms over finite fields and reconstructing multivariate rational functions. The framework employs computational graphs, known as dataflow graphs, to combine basic building blocks into complex algorithms. This allows to easily implement a wide range of methods over finite fields in high-level languages and computer algebra systems, without being concerned with the low-level details of the numerical implementation. This approach sidesteps the appearance of large intermediate expressions and can be massively parallelized. We present applications to the calculation of multi-loop scattering amplitudes, including the reduction via integration-by-parts identities to master integrals or special functions, the computation of differential equations for Feynman integrals, multi-loop integrand reduction, the decomposition of amplitudes into form factors, and the derivation of integrable symbols from a known alphabet. We also release a proof-of-concept C++ implementation of this framework, with a high-level interface in MATHEMATICA.

arXiv:1905.08019v2 [hep-ph] 17 Jul 2019

Contents

1	Introduction	3
2	Finite fields and functional reconstruction	6
2.1	Finite fields and rational functions	6
2.2	Multivariate functional reconstruction	7
2.3	Parallelization	11
3	Dataflow graphs	12
3.1	Graphs as numerical procedures	12
3.2	Learning nodes	14
3.3	Subgraphs	14
4	Numerical algorithms over finite fields	15
4.1	Evaluation of rational functions	15
4.2	Dense and sparse linear solvers	16
4.3	Linear fit	20
4.4	Basic operations on lists and matrices	22
4.5	Laurent expansion	23
4.6	Algorithms with no input	24
5	Reduction of scattering amplitudes	24
5.1	Integration-by-parts reduction to master integrals	25
5.2	Reduction to special functions and Laurent expansion in ϵ	28
6	Differential equations for master integrals	29
6.1	Reconstructing differential equations	30
6.2	Differential equations in ϵ -form	31
6.3	Differential equations with square roots	32
7	Integrand reduction	33
7.1	Integrand reduction via linear fits	34
7.2	Choice of an integrand basis	36
7.3	Writing the integrand	38
8	Decomposition of amplitudes into form factors	39
9	Finding integrable symbols from a known alphabet	40
10	Proof-of-concept implementation	42
10.1	Parallel execution	46
11	Conclusions	47
	Appendix A Mutability of graphs and nodes	48
	Appendix B Further observations on IBP identities	48

1 Introduction

Scientific theoretical predictions often rely on complex algebraic calculations. This is especially true in high energy physics, where current and future experiments demand precise predictions for complex scattering processes. One key ingredient for making these predictions are scattering amplitudes in perturbative quantum field theory. The complexity of these predictions depends on several factors, most notably the loop order, where higher loop orders are required for higher precision, the number of scattering particles involved, and the number of independent physical scales describing the process.

A major bottleneck in many analytic predictions is the appearance of large expressions in intermediate stages of the calculation. These can be orders of magnitude more complicated than the final result. Large analytic cancellations often happen in the very last stages of a calculation. While computer algebra extraordinarily enhances our capability of making such predictions, due to the reasons above, it needs to be complemented with more effective techniques when dealing with the most challenging computations.

One can trivially observe that the mentioned bottleneck is not present in numerical calculations with fixed precision, where every intermediate result is a number (or a list of numbers). However, in some fields, high-energy physics being one of them, analytic calculations provide more valuable results – since they can provide a more accurate numerical evaluation, and the possibility of further checks, studies and manipulations – and in some cases our only reliable way of obtaining them.

An effective method for sidestepping the bottleneck of complex intermediate expressions consists of reconstructing analytic expressions from numerical evaluations. This can be effectively used in combination with *finite fields*, i.e. numerical fields with a finite number of elements. In particular, we may choose fields whose elements can be represented by machine size integers, where basic operations can be done via modular arithmetic. Numerical operations over these fields are therefore relatively fast, but also exact, while they avoid the need of using multi-precision arithmetic, which is computationally expensive. Full analytic expressions for multivariate rational functions can then be obtained, using *functional reconstruction* techniques, from several numerical evaluations with different input values and, if needed, over several finite fields. Thanks to these algorithms, the problem of computing a rational function is reduced to the problem of providing an efficient numerical evaluation of it over finite fields. This implies that they can be applied to a very broad range of problems. Moreover, numerical evaluations can be massively parallelized, taking full advantage of the available computing resources.

Finite fields have been used by computer algebra systems for a long time. In high-energy physics, they were introduced in ref. [1] for the solution of (univariate) integration-by-parts (IBP) identities. In ref. [2] we developed a multivariate reconstruction algorithm which is suitable for complex multi-scale problems and showed how to apply it to other techniques in high-energy physics, such as integrand reduction [3–8] and generalized unitarity [9–12]. Since then, functional reconstruction techniques based on evaluations over finite fields have been successfully employed in several calculations which proved to be beyond the reach of conventional computer algebra systems, with the available computing resources (see e.g. refs [13–21] for some notable examples).

Despite the remarkable results which have already been obtained with functional reconstruction techniques, there are still some obstacles which prevent a more widespread usage of them. A first one is the lack of a public implementation of functional reconstruction tech-

niques suitable for arbitrary multivariate rational functions.¹ A second obstacle is the need of providing an efficient numerical implementation of the functions to be reconstructed, which is typically best done in statically compiled low-level languages, such as C, C++ or FORTRAN. In this paper, we try to address both these problems.

Let us assume a functional reconstruction algorithm is available, and consider the problem of providing an efficient numerical evaluation of an algorithm representing a rational function over finite fields. The first possibility is obviously low-level coding. This offers great performance and flexibility, but it is also hard and time-consuming to program and therefore it limits the usability of these techniques, especially if compared with the ease of use of computer algebra systems.

Another strategy consists in coding up some algorithms in low-level languages and providing interfaces in higher level languages and computer algebra systems. This combines the efficiency of low-level languages with the ease of use of high-level ones. As an example, consider the problem of solving a linear system of equations with parametric rational entries. Most computer algebra systems have dedicated built-in procedures for this. One could build another procedure, with a similar interface, which instead sends the system to a C/C++ code, which in turn solves it numerically several times and reconstructs the analytic solution from these numerical evaluations. For the user of the procedure, there is very little difference (except for performance) with respect to using the built-in procedure. Unfortunately, this strategy strongly limits the flexibility of functional reconstruction, since one is limited to use a set of hardcoded algorithms. Moreover, these algorithms often solve only an intermediate step of a more complex calculation needed by a scientific prediction. For instance, in most cases, one needs to substitute the solution of a linear system into another expression and then perform other operations or substitutions before obtaining the final result. Significant analytic simplifications often occur at the very last steps of the calculation, making thus the reconstruction of the intermediate steps a highly inefficient strategy. We thus need something which is much more flexible and applicable to a wider variety of problems.

One can observe that many different complex calculations share common building blocks. For instance, many calculations involve the solution of one or more linear systems, changes of variables, linear substitutions, and so on, in intermediate stages. These intermediate calculations, however, need to be combined in very different ways, depending on the specific problem an algorithm is meant to solve. Building on this observation, we propose a strategy which allows to easily combine these basic building blocks into arbitrarily complex calculations.

In this paper, we introduce a framework, that we call FINITEFLOW, which allows to easily define complicated numerical algorithms over finite fields, and reconstruct analytic expressions out of numerical evaluations. The framework consists of three main components. The first component is a set of basic numerical algorithms, efficiently implemented over finite fields in a low-level language. These include algorithms for solving linear systems, linear fits, evaluating polynomials and rational functions, and many more. The second component is a system for combining these basic algorithms, used as building blocks, into arbitrarily more complex ones. This is done using *dataflow graphs*, which provide a graphical representation of a complex calculation. Each *node* in the graph represents a basic algorithm. The inputs of each of these algorithms are in turn chosen to be the outputs of other basic algorithms, represented by other nodes. This provides a simple and effective way of defining complicated algebraic calcu-

¹During advanced stages of preparation of this work, an implementation of a sparse multivariate reconstruction algorithm was published [22]. In this paper we describe instead a dense reconstruction algorithm.

lations, by combining basic building blocks into complex algorithms, without the need of any low-level coding. Indeed, this framework can be more easily used from interfaces in high-level languages and computer algebra systems. Dataflow graphs can be numerically evaluated and their output represents – in our framework – a list of rational functions. Numerical evaluations with different inputs can be easily performed in parallel, in a highly automated way. Indeed, this defines an algorithm-independent strategy for exploiting computing resources consisting of several cores, nodes, or machines. The third and last component consists of functional reconstruction algorithms, which are used to reconstruct analytic formulas out of the numerical evaluations (which in turn, as stated, may be represented by a graph). We propose here an improved version of the reconstruction algorithms already presented in [2].

The idea of using dataflow graphs for defining a numerical calculation is not new. For instance, they are notably used in the popular TENSORFLOW library [23], in the context of machine learning and neural networks. Although in this paper, we are interested in a very different application, one can point out a few similarities. For instance, the TENSORFLOW library allows to define complex functions (which, in that case, often represent neural networks) from high-level languages, which then need to be efficiently evaluated several times. To the best of our knowledge, this paper describes for the first time an application of dataflow graphs for the purpose of defining (rational) numerical algorithms over finite fields, to be used in combination with functional reconstruction techniques. In particular, we will show, by providing several examples, that they are suited for solving many types of important problems in high-energy physics.

With this paper, we also release a proof-of-concept C++ implementation of this framework, which includes a MATHEMATICA interface. This code has already been used in a number of complex analytic calculations, including some recently published cutting-edge scientific results [14, 17, 21], and we thus think its publication can be highly beneficial. We stress that FINITEFLOW is not meant to provide the solution of any specific scientific problem, but rather a framework which can be used for solving a wide variety of problems. We also provide public codes with several packages and examples of applications of FINITEFLOW to very common problems in high-energy physics, which can be easily adapted to similar problems as well.

The paper is organized as follows. In section 2 we review some basic concepts about finite fields and rational functions, and we describe an efficient functional reconstruction algorithm for multivariate functions. In section 3 we describe our system for defining numerical algorithms, based on dataflow graphs. In section 4 we describe the implementation of several numerical algorithms over finite fields, which are the basic building blocks of the dataflow graphs representing a more complex computation. In the next sections, we describe the application of this framework to several problems in high-energy physics. In section 5 we discuss the reduction of scattering amplitudes to master integrals or special functions, as well as the Laurent expansion in the dimensional regulator. In section 6 we discuss the application to differential equations for computing master integrals. In sections 7 and 8 we discuss multi-loop integrand reduction and the decomposition of amplitudes into form factors respectively. In section 9 we talk about the derivation of integrable symbols from a known alphabet. Finally, in section 10 we give some details about our public proof-of-concept implementation, and in section 11 we draw our conclusions.

2 Finite fields and functional reconstruction

In this section, we set some notation by reviewing well-known facts about finite fields and rational functions. We also describe a multivariate reconstruction algorithm based on numerical evaluations over finite fields. The latter is based on the one described in [2] with a few modifications and improvements. A slightly more thorough treatment of the subject, which uses a notation compatible with the one of this paper, can be found in ref. [2] (in particular, in sections 2, 3 and Appendix A of that reference).

2.1 Finite fields and rational functions

Finite fields are mathematical fields with a finite number of elements. In this paper, we are only concerned with the simplest and most common type of finite field, namely the set of integers modulo a prime p , henceforth indicated with \mathbb{Z}_p . In general, for any positive integer n , we call \mathbb{Z}_n the set of non-negative integers smaller than n . All basic rational operations in \mathbb{Z}_n , except division, can be trivially defined using modular arithmetic. One can also show that if $a \in \mathbb{Z}_n$ and $\gcd(a, n) = 1$ then a has a unique inverse in \mathbb{Z}_n . In particular, if $n = p$ is prime, an inverse exists for any non-vanishing element of \mathbb{Z}_p , hence any rational operation is well defined. This also defines a map between rational numbers $q = a/b \in \mathbb{Q}$ and \mathbb{Z}_n , for any rational whose denominator b is coprime with n . It also implies that any numerical algorithm which consists of a sequence of rational operations can be implemented over finite fields \mathbb{Z}_p . In particular, polynomials and rational functions are well defined mathematical objects.

Given a set of variables $\mathbf{z} = \{z_1, \dots, z_n\}$ and a numerical field \mathbb{F} , one can define polynomial and rational functions of \mathbf{z} over \mathbb{F} . More in detail, any list of exponents $\alpha = \{\alpha_1, \dots, \alpha_n\}$, defines the monomial

$$\mathbf{z}^\alpha = \prod_{j=1}^n z_j^{\alpha_j}. \quad (2.1)$$

Polynomials over \mathbb{F} have a unique representation as linear combinations of monomials

$$p(\mathbf{z}) = \sum_{\alpha} c_{\alpha} \mathbf{z}^{\alpha}, \quad (2.2)$$

with coefficients $c_{\alpha} \in \mathbb{F}$. Rational functions are ratios of two polynomials

$$f(\mathbf{z}) = \frac{\sum_{\alpha} n_{\alpha} \mathbf{z}^{\alpha}}{\sum_{\alpha} d_{\alpha} \mathbf{z}^{\alpha}}, \quad (2.3)$$

with $n_{\alpha}, d_{\alpha} \in \mathbb{F}$. Notice that the representation of $f(\mathbf{z})$ in Eq. (2.3) is not unique. A unique representation can, however, be obtained by requiring numerator and denominator to have no common polynomial factor, and fixing a convention for the normalization on the coefficients n_{α}, d_{α} . We find that a useful convention is setting $d_{\min(\alpha)} = 1$, where $\mathbf{z}^{\min(\alpha)}$ is the smallest monomial appearing in the denominator with respect to a chosen monomial order. Using this convention, the constant term in the denominator, if present, is always equal to one.

An important result in modular arithmetic is Wang's *rational reconstruction* algorithm [24, 25] which allows, in some cases, to invert the map between \mathbb{Q} and \mathbb{Z}_n . More in detail, given the image $z \in \mathbb{Z}_n$ of a number $q = a/b \in \mathbb{Q}$, Wang's algorithm successfully reconstructs q if n is large enough with respect to the numerator and the denominator of the rational number – more precisely if and only if $|a|, |b| < \sqrt{n/2}$. Hence, if a prime p is sufficiently large, one can

successfully reconstruct a rational number from its image in \mathbb{Z}_p . However, our main reason for using finite fields is the possibility of performing calculations efficiently using machine size integers, which on most modern machines can have a size of 64 bits. This requirement forces us to use primes such that $p < 2^{64}$. One can overcome this limitation by means of the Chinese remainder theorem, which allows to deduce a number $a \in \mathbb{Z}_n$ from its images $a_i \in \mathbb{Z}_{n_i}$ if the integers n_i have no common factors. Hence, given a sequence of primes $\{p_1, p_2, \dots\}$, from the image of a rational number over several prime fields $\mathbb{Z}_{p_1}, \mathbb{Z}_{p_2}, \dots$ one can deduce the image of the same number over $\mathbb{Z}_{p_1 p_2 \dots}$. Once the product of the selected primes is large enough, Wang’s reconstruction algorithm will be successful.

The functional reconstruction algorithm we will describe in the next section can be performed over any field, but in practice, it will only be implemented over finite fields. The coefficients of the reconstructed function (i.e. n_α, d_α appearing in Eq. (2.3)) are then mapped over the rational field using Wang’s algorithm and checked numerically against evaluations of the function over other finite fields. If the check is unsuccessful, we proceed with reconstructing the function over more finite fields \mathbb{Z}_{p_i} , and combine them using the Chinese remainder theorem as explained above, in order to obtain a new result over \mathbb{Q} . The algorithm terminates when the result over \mathbb{Q} agrees with numerical checks over finite fields which have not been used for the reconstruction.

2.2 Multivariate functional reconstruction

We now turn to the, so called, *black box interpolation problem*, i.e. the problem of inferring, with very high probability, the analytic expression of a function from its numerical evaluations. We assume to have a numerical procedure for evaluating an n -variate rational function f , whose analytic form is not known. More in detail, the procedure takes as input numerical values for \mathbf{z} and a prime p and returns the function evaluated at \mathbf{z} over the finite field \mathbb{Z}_p ,

$$(\mathbf{z}, p) \longrightarrow \boxed{f} \longrightarrow f(\mathbf{z}) \bmod p. \tag{2.4}$$

We also allow the possibility for this procedure to fail the evaluation. We call this evaluation points *bad points* or *singular points*. Notice that these do not necessarily correspond to a singularity in the analytic expression of the function, but also to spurious singularities in intermediate steps of the procedure, or to any other interference with the possibility of evaluating the function with the implemented numerical algorithm. When this happens, the singular evaluation point is simply replaced with a different one. We stress, however, that the occurrence of such cases is extremely unlikely for a realistic problem, provided that the evaluation points are chosen with care (we will expand on this later).

A functional reconstruction algorithm aims to identify the monomials appearing in the analytic expression of the function as in Eq. (2.3), and the value of their coefficients n_α, d_α . The basic reconstruction algorithm we discuss in this section is based on a strategy already proposed in ref. [2]. However, we find it is useful to briefly summarize it here in order to point out a few modifications and improvements, and also because the discussion below will benefit from having a rough knowledge of how the functional reconstruction works.

For univariate polynomials, our reconstruction strategy is based on Newton’s polynomial

representation [26]

$$\begin{aligned} f(z) &= \sum_{r=0}^R a_r \prod_{i=0}^{r-1} (z - y_i) \\ &= a_0 + (z - y_0) \left(a_1 + (z - y_1) \left(a_2 + (z - y_2) \left(\cdots + (z - y_{R-1}) a_R \right) \right) \right), \end{aligned} \quad (2.5)$$

where R is the total degree, and y_0, y_1, y_2, \dots are a sequence of distinct numbers. One can easily check that, with this representation, any coefficient a_r can be determined from the knowledge of the value of the function at $z = y_r$ and from the coefficients a_j with $j < r$. In particular, it does not require the knowledge of the total degree R . This allows to recursively reconstruct the coefficients a_r of the polynomial, starting from a_0 which is determined by $f(y_0)$. If the total degree of the polynomial is not known, the termination criterion of the reconstruction algorithm is the agreement between new evaluations of the function f and the polynomial defined by the coefficients reconstructed so far. In some cases, the total degree, or an upper bound to it, is known a priori (see e.g. when this is used in the context of a multivariate reconstruction) and therefore one can terminate the reconstruction as soon as this bound is reached. After the polynomial is reconstructed, it is converted back into a canonical representation.

For univariate rational functions, we distinguish two cases. The first case, which will be useful in the context of multivariate reconstruction, is when the total degree of the numerator and the denominator of the function are known and the constant term in the denominator does not vanish. This means, remembering the normalization convention we introduced in section 2.1, that we can parametrize the function as

$$f(z) = \frac{\sum_{j=0}^R n_j z^j}{1 + \sum_{j=1}^{R'} d_j z^j} \quad (2.6)$$

for known total degrees R and R' . Given a sequence of distinct numbers y_0, y_1, y_2, \dots , one can build a linear system of equations for the coefficients n_j and d_j by evaluating the function f at $z = y_k$, namely

$$\sum_{j=0}^R n_j y_k^j - \sum_{j=1}^{R'} d_j y_k^j f(y_k) = f(y_k). \quad (2.7)$$

This strategy is even more convenient when a subset of the coefficients is already known since it allows to significantly reduce the number of needed evaluations of the function (this will also be important later).

For the more general case where we do not have any information on the degrees of the numerator and the denominator of the function, we use Thiele's interpolation formula [26],

$$\begin{aligned} f(z) &= a_0 + \frac{z - y_0}{a_1 + \frac{z - y_1}{a_2 + \frac{z - y_2}{\cdots + \frac{z - y_{r-1}}{a_N}}}} \\ &= a_0 + (z - y_0) \left(a_1 + (z - y_1) \left(a_2 + (z - y_2) \left(\cdots + \frac{z - y_{N-1}}{a_N} \right)^{-1} \right)^{-1} \right)^{-1}, \end{aligned} \quad (2.8)$$

where y_0, y_1, \dots is, once again, a sequence of distinct numbers. Thiele's formula is the analogous for rational functions of Newton's formula, and indeed it can be used in order to interpolate a univariate rational function using the same strategy we illustrated for the polynomial case. Similarly as before, the result is converted into a canonical form after the reconstruction.

The reconstruction of multivariate polynomials is performed by recursively applying Newton's formula. Indeed a multivariate polynomial in $\mathbf{z} = \{z_1, \dots, z_n\}$ can be seen as a univariate polynomial in z_1 whose coefficients are multivariate polynomials in the other variables z_2, \dots, z_n ,

$$f(z_1, \dots, z_n) = \sum_{r=0}^R a_r(z_2, \dots, z_n) \prod_{i=0}^{r-1} (z_1 - y_i). \quad (2.9)$$

For any fixed numerical value of z_2, \dots, z_n one can apply the univariate polynomial reconstruction algorithm in z_1 to evaluate the coefficients a_r . This means that the problem of reconstructing an n -variate polynomial is reduced to the one of reconstructing an $(n - 1)$ -variate polynomial. Hence we apply this strategy recursively until we reach the univariate case, which we already discussed. The result is then converted into the canonical form of Eq. (2.2).

Before moving to the case of multivariate rational functions, it is worth making a few observations on the choice of the sequence of evaluation points y_0, y_1, \dots which appear in all the previous algorithms. We want to make a choice which does not interfere with our capability of evaluating the function f – which may have singularities both in its final expression and in intermediate stages of its numerical evaluation – and of inverting the relations for obtaining Thiele's coefficients. While making a choice which works for any function is clearly impossible, in practice we can easily make one which almost always works in realistic cases. This is done by choosing as y_0 a relatively large and random-like integer in \mathbb{Z}_p , where common functions are extremely unlikely to have singularities. We then increase the integer by a relatively large constant δ for the next points, i.e. $y_{i+1} = y_i + \delta \pmod p$. In the multivariate case, we use a different starting point y_0 and a different constant δ for each variable. Heuristically we find that, with this strategy, especially when using 64-bit primes, one can reasonably expect to find no singular point even in millions of evaluations.

We finally discuss the more complex problem of reconstructing a multivariate rational function $f = f(\mathbf{z})$. We first observe that the reconstruction is much simpler when the constant term in the denominator is non-vanishing since this unambiguously fixes the normalization of the coefficients. As suggested in ref. [27], we can force any function to have this property by shifting its arguments by a constant vector $\mathbf{s} = \{s_1, \dots, s_n\}$ and reconstruct $f(\mathbf{z} + \mathbf{s})$ instead. In practice, by default, we find it is convenient to always shift arguments by a vector \mathbf{s} such that any function coming from a realistic problem is unlikely to be singular in $\mathbf{z} = \mathbf{s}$. The criteria for the choice of \mathbf{s} are similar to the ones for choosing the sample points, i.e. choosing relatively large and random-like numbers in \mathbb{Z}_p . The result is shifted back to its original arguments after the full reconstruction over a finite field \mathbb{Z}_p is completed (note that this detail differs from what is proposed in ref.s [2, 27]). Hence, in the following, we assume that the function f has a non-vanishing constant term in the denominator, which by our choice of normalization is equal to one.

The key ingredient of the algorithm, which was also proposed in ref. [27], is the introduction of an auxiliary variable t which is used to rescale all the arguments of f . This defines

the function $h = h(t, \mathbf{z})$, which takes the form

$$h(t, \mathbf{z}) \equiv f(t \mathbf{z}) = \frac{\sum_{r=0}^R p_r(\mathbf{z}) t^r}{1 + \sum_{r=1}^{R'} q_r(\mathbf{z}) t^r}. \quad (2.10)$$

In other words, $h(t, \mathbf{z})$ is a univariate rational function in t , whose coefficients p_r and q_r are multivariate homogeneous polynomials of total degree r in \mathbf{z} . This allows to reconstruct $f(\mathbf{z}) = h(1, \mathbf{z})$ by combining the algorithms discussed above for univariate rational functions and multivariate polynomials. In practice, we start with a univariate reconstruction in t for fixed values of \mathbf{z} using Thiele's formula, in order to get the total degree of numerator and denominator. This allows to check that the denominator has indeed a non-vanishing constant term. The knowledge of the total degree also allows to use the system-solving strategy for the next reconstructions in t . We also perform a univariate reconstruction of the unshifted function f in each variable z_j for fixed values of all the other variables. The minimum degrees in each variable are used to factor out polynomial prefactors in the numerator and denominator of the function, which can significantly reduce the number of required evaluations (note that it is essential that this is done before shifting variables since after the shift any realistic function is unlikely to have monomial prefactors). The maximum degrees are used to provide, together with the total degree r of each polynomial p_r and q_r , the possibility of terminating the polynomial reconstructions in the interested variables earlier. They are also used in order to estimate a suitable set of sample points for reconstructing the function before performing the evaluations, as we will explain when discussing the parallelization strategy in section 2.3. We then proceed with using the system-solving strategy for univariate rational functions, reconstructing $h(t, \mathbf{z})$ as a function of t for any fixed numerical value of \mathbf{z} . This provides an evaluation of the polynomials p_r and q_r at \mathbf{z} . By repeating this for several values of \mathbf{z} , we reconstruct these multivariate polynomials using Newton's formula recursively.

A few observations are in order. First, because the polynomials p_r and q_r are homogeneous, we can set $z_1 = 1$ and restore its dependence at the end. This makes up for having introduced the auxiliary variable t . Moreover, each reconstruction in t provides an evaluation of all the polynomial coefficients at the same time. For this reason, for each \mathbf{z} we cache the reconstructed coefficients so that we can reuse the evaluations in several polynomial reconstructions. As for the reconstruction of the polynomials themselves, we proceed from the ones with a lower degree to the ones of higher degree (this detail is also different from what is presented in ref. [2]). This way the polynomials with a lower degree, which can be reconstructed with fewer evaluations, become known earlier and can thus be removed from the system of equations in Eq. (2.7) when reconstructing the ones with higher degrees. This makes the system of equations for higher-degree polynomial coefficients smaller, and hence it further reduces the number of needed evaluations. As already mentioned, we also use the information on the total degree r of each polynomial, as well as the maximum degree with respect to each variable, in order to terminate the polynomial reconstructions earlier, when possible.

When combining all these ingredients, we find that the number of evaluations we need for the reconstruction is comparable (if not better) to the one we would need by writing a general ansatz based on the degrees of the numerator and the denominator of the function (both the total ones and the ones with respect to each variable). However, while the ansatz-based approach is impractical for complicated multivariate functions since it requires to solve huge dense systems of equations, the method presented here is instead able to efficiently reconstruct very complex functions depending on several variables. It has indeed been applied to a large number of examples, some of which have been mentioned in the introduction.

Finally, we point out that so far we only discussed single-valued functions, but in the most common cases the output of an algorithm will actually be a list of functions

$$\mathbf{f}(\mathbf{z}) = \{f_1(\mathbf{z}), f_2(\mathbf{z}), \dots\}. \quad (2.11)$$

In this case, the reconstruction proceeds as described above considering one element of the output at the time. However, for each functional evaluation, the whole output, or a suitable subset of it, is cached (more details on our caching strategy are discussed in section 10) so that the same evaluations can be reused for the reconstruction of different functions $f_j(\mathbf{z})$.

2.3 Parallelization

A well-known advantage of functional reconstruction techniques is the possibility to extensively parallelize the algorithm.

The most important step which can be parallelized is the evaluation of the function. Since numerical evaluations are independent of each other, they can be run in parallel over different threads, nodes, or even on different machines.

Building an effective parallelization strategy is actually easier for the multivariate case. As discussed above, the multivariate reconstruction begins with a univariate reconstruction in t of the function $h(t, \mathbf{z})$ in Eq. (2.10), and univariate reconstructions in each variable z_j for fixed values of all the other ones. This amounts, for an n -variate problem, to $n + 1$ univariate reconstructions, which being independent of each other can be all run in parallel. These univariate reconstructions are significantly faster than a multivariate one and provide valuable information for the multivariate reconstruction. After this step we use this information to determine a suitable set of evaluation points for the reconstruction of each function in the output of the algorithm, assuming the result is a generic function constrained by the degrees found in the univariate fits. While this might result in building a set of evaluation points which is slightly larger than needed, it allows to obtain a list of sample points which can be independently evaluated before starting any multivariate reconstruction. Any performance penalty, due to this oversampling of the function, is very small compared to what we gain from the possibility of parallelizing the evaluations. Therefore, this list of points can be split according to the available computing resources and evaluated in parallel over as many threads and cores as possible.

The main advantage of this parallelization strategy is the relative ease of implementation since it requires minimal synchronization (each thread just needs to evaluate all the points assigned to it and wait for the others to finish), and the fact that it does not depend on the specific numerical algorithm which is implemented.

After the evaluations have completed, they are collected and used for the multivariate reconstruction algorithm described above, except that the calls to the numerical “black box” procedure are now replaced by a lookup of its values in the set of cached evaluations.

In building the list of evaluation points, one may initially assume that a given number n_p of primes will be needed for the reconstruction over \mathbb{Q} (typically, one will start with the choice $n_p = 1$), and that additional primes will only be used for a small number of evaluations, for the purpose of checking the result. If the rational reconstruction described in section 2.1 fails these checks, points using additional primes will be added to the list and another evaluation step will be performed for these.

We now turn to the univariate case. Since building an effective and clean parallelization strategy here is significantly harder than for the multivariate case and in general, one does not

need too many evaluations for univariate reconstructions, by default we don't perform any parallelization in the univariate case. Indeed, the strategy illustrated above would require us to perform a univariate reconstruction over a finite field before performing any parallelization, in order to obtain information on the degree of the result. For the univariate case, however, this task is of comparable complexity than performing a complete reconstruction over \mathbb{Q} . Despite this, if needed, we can still parallelize the evaluations in a highly automated way as follows. We start by making a guess on the maximum degrees of numerator and denominator and build a set of evaluation points based on this assumption. Then we perform the evaluations in parallel, as before. After this, we proceed with the reconstruction using the cached evaluations. If during the reconstruction we realize we need more evaluation points, we make a more conservative guess of the total degrees and proceed again with the evaluation (in parallel) of the additional points needed. This can be done automatically, by gradually increasing the maximum degree by a given amount in each step. We proceed this way until the reconstruction is successful. Obviously, making an accurate guess of the total degrees may not be easy. While making a conservative choice of a high degree might result in too many evaluations, choosing a total degree which is too low will cause the reconstruction to fail and it will create additional overhead in launching the parallel tasks for evaluating the additional points until the successful reconstruction. This method also requires some additional input from the user of the reconstruction algorithm, which needs to provide these guesses, since one cannot obviously make a choice which is good for any problem. For these reasons, we usually prefer to avoid parallelization in univariate reconstruction, but it is still important to know that a parallelization option is available for these cases as well.

Another step which can be, to some extent, parallelized, is the reconstruction itself. As mentioned, in the most common cases, the output of our algorithm is not a single function but a list of functions. Since the reconstructions of different functions from a set of numerical evaluations are independent of each other, they can also be run in parallel. Even if this is generally not as important as the parallelization of the functional evaluations, which are the typical bottleneck, it can still yield a sizeable performance improvement.

3 Dataflow graphs

In this section, we describe one of the main novelties introduced in this paper, namely a method for building numerical algorithms over finite fields using a special kind of computational graphs, known as *dataflow graphs*.

The algorithms described in the previous sections reduce the problem of computing any (multivariate and multivalued) rational function to the one of providing a numerical implementation of it, over finite fields \mathbb{Z}_p . The goal of the method described in this section is providing an effective way of building this implementation, characterized by good flexibility, performance, and ease of use.

3.1 Graphs as numerical procedures

Dataflow graphs are directed acyclic graphs, which can be used to represent a numerical calculation. The graph is made of nodes and arrows. The *arrows* represent data (i.e. numerical values in our case) and the *nodes* represent algorithms operating on the (incoming) data received as input and producing (outgoing) data as output. In the following, we describe a simplified type of dataflow graphs which we use in our implementation.

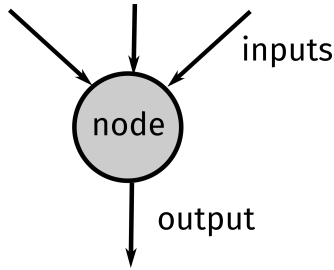


Figure 1: A node in a dataflow graph, where arrows represent lists of values and nodes represent numerical algorithms. In our implementation, a node can take zero or more incoming arrows as input and has exactly one outgoing arrow as output.

In our case, an *arrow* represents a *list of values*. A *node* represents a *basic numerical algorithm*. A node can take zero or more incoming arrows (i.e. lists) as input and has exactly one outgoing arrow² (i.e. one list) as output (see fig. 1). For simplicity, we also require that each list (represented by an arrow) has a well-defined length which cannot change depending on the evaluation point. We also understand that nodes can also contain metadata with additional information needed to define the algorithm to be executed.

Typically nodes encode common, basic algorithms (e.g. the evaluation of rational functions, the solution of linear systems, etc...) which are implemented, once and for all, in a low-level language such as C++. We will give an overview of the most important ones in section 4. Complex algorithms are defined by combining these nodes, used as building blocks, into a computational graph representing a complete calculation, where the output of a building block is used as input for others. This way complex algorithms are easily built without having to deal with the low-level details of their numerical implementation. The graph can indeed be built from a high-level language, such as PYTHON or MATHEMATICA. Several explicit examples will be provided in the next sections.

In each graph, there are two special nodes, namely the *input node* and the *output node*. The input node does not represent any algorithm, but only the list of input variables \mathbf{z} of the graph. The output node can be any node of the graph and represents, of course, its output. A dataflow graph thus defines a numerical procedure which takes as input the variables \mathbf{z} represented by the input node and returns a list of values which is the output of the output node.

Graphs are evaluated as follows. First, every time we define a node, we assign to it an integer value called *depth*. The depth of a node is the maximum value of the depths of its inputs plus one. The depth of the input node is zero, by definition. When an output node is specified, we recursively select all the nodes which are needed as inputs in order to evaluate it, and we sort this list by depth. We then evaluate all the nodes from lower to higher depths and store their output values to be used as inputs for other nodes. Once the output node has been evaluated, its output is returned by the evaluation procedure.

² In the graphical representations in this paper, if there are two or more outgoing arrows for a node, we understand that they all represent the same list.

3.2 Learning nodes

As we already mentioned, each node has exactly one list of values as output, and the length of this list is not allowed to change depending e.g. on the evaluation point. However, for some algorithms, we cannot know the length of the output at the moment the numerical procedure is defined.

Consider, as an example, a node which solves a linear system of equations. The length of the output of such a node depends on whether the system is determined or undetermined and on its rank. This information is usually not known a priori but it must be *learned* after the system is defined. In this case, it can easily be learned by solving the system numerically a few times.

For this reason, we allow nodes to have a *learning phase*. The latter is algorithm-dependent and typically consists of a few numerical evaluations used by a node in order to properly define its output. Hence, the output of these nodes can be used as input by other nodes only after the learning phase is completed (since, before that, their output cannot be defined at all).

More algorithms which require a learning phase will be discussed later.

3.3 Subgraphs

An important feature which makes this framework more powerful and usable in realistic problems is the possibility of defining nodes in which one can embed other graphs.

Consider a graph G_1 with a node N which embeds a graph G_2 . We say that G_2 is a *subgraph*. Typically, the node N will need to evaluate the subgraph G_2 a number of times in order to produce its output.

The simplest case of a subgraph is when the node N takes one list as input, passes the same input to G_2 in order to evaluate it, and then returns the output of G_2 . This case, which we call *simple subgraph*, is equivalent to having the nodes of G_2 attached to the input node of N inside the graph G_1 directly, but it can still be useful in order to organize more cleanly some complicated graphs.

Another interesting example, which we call *memoized subgraph*, can be beneficial when parts of the calculation are independent of some of the variables. This type of subgraph effectively behaves the same way as the simple subgraph described above, except that it remembers the input and the output of the last evaluation. If the subgraph needs to be evaluated several times in a row with the same input, the memoized subgraph simply returns the output it has stored. This is particularly useful when combined with the Laurent expansion, the subgraph fit, or the subgraph multi-fit algorithms. We will give a description of these later in this paper, but for now, it suffices to know that they require to evaluate a dataflow graph several times for fixed values of a subset of the variables. In such cases, one may not wish to evaluate every time the parts of a graph which only depend on the variables which remain fixed for several evaluations. One can thus optimize away these evaluations by embedding the appropriate parts of the graph in a memoized subgraph.

One more useful type of subgraph is a *subgraph map*. This takes an arbitrary number of lists of length n as input, where n is the number of input parameters for G_2 . The graph G_2 is then evaluated for each of the input lists, and the outputs are chained together and returned. This is useful when the same algorithm needs to be evaluated for several inputs.

There are however other interesting cases, where the node N requires to evaluate G_2 several times and perform non-trivial operations on its output. Some useful examples are

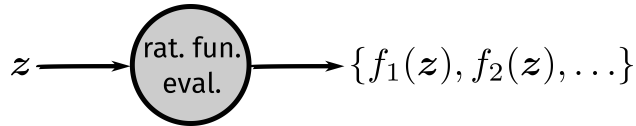


Figure 2: A node representing the evaluation of a list of rational functions. It takes one list \mathbf{z} as input, interpreted as the list of arguments of the functions, and returns the values of the functions evaluated at \mathbf{z} .

given at the end of section 4.3 and in section 4.5.

4 Numerical algorithms over finite fields

In this section, we discuss several basic, numerical algorithms which can be used as nodes in a graph. These are best implemented in a low-level language such as C++ for efficiency reasons. In later sections, we will then show how to combine these basic building blocks into more complex algorithms which are relevant for state-of-the-art problems in high-energy physics.

4.1 Evaluation of rational functions

Most of the algorithms we are interested in have some kind of analytic input, which can be cast in the form of one or more lists of polynomials or rational functions. The numerical evaluation of rational functions is, therefore, one of the most ubiquitous and important building blocks in our graphs. These nodes take as input one list of values \mathbf{z} and return a list of rational functions $\{f_j(\mathbf{z})\}$ evaluated at that value, as schematically illustrated in fig. 2.

Polynomials are efficiently evaluated using the well known Horner scheme. Given a univariate polynomial

$$p(z) = \sum_{j=0}^R c_j z^j, \quad (4.1)$$

Horner's method is based on expressing it as

$$p(z) = c_0 + z (c_1 + z (c_2 + \cdots z (c_{R-1} + z c_R))). \quad (4.2)$$

This formula only has R multiplications and R additions for a polynomial of degree R , and it can be easily obtained from the canonical representation in Eq. 4.1. Therefore, it is a great compromise between ease of implementation and efficiency.

For multivariate polynomials, Horner's scheme is applied recursively in the variables. In practice, we use an equivalent but non-recursive implementation and we store all the polynomial data (i.e. the integer coefficients c_j and the meta-information about the total degrees of each sub-polynomial) in a contiguous array of integers.

Rational functions are obviously computed as ratios of two polynomials. If the denominator vanishes for a specific input, the evaluation fails and yields a singular point.

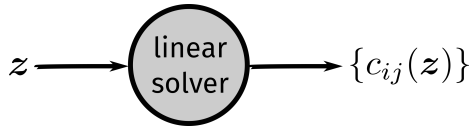


Figure 3: A node representing a linear solver. It takes as input a list of parameters \mathbf{z} and returns the coefficients of the solution defined in Eq. (4.5) and (4.6).

4.2 Dense and sparse linear solvers

A wide variety of algorithms involves solving one or more linear systems at some stage of the calculation. Moreover, the solution of these systems is often the main bottleneck of the procedure, hence having an efficient numerical linear solver is generally very important.

In general, consider a $n \times m$ linear system with parametric rational entries in the parameters \mathbf{z} ,

$$\sum_{j=1}^m A_{ij} x_j = b_i, \quad (i = 1, \dots, n), \quad (4.3)$$

with

$$A_{ij} = A_{ij}(\mathbf{z}), \quad b_i = b_i(\mathbf{z}). \quad (4.4)$$

This is defined by the matrix $A = A(\mathbf{z})$, the vector $b = b(\mathbf{z})$, and the set of m variables or unknowns $\{x_j\}$. We assume there is a total ordering between the unknowns, $x_1 \succ x_2 \succ \dots \succ x_m$. Borrowing from a language commonly used in the context of IBP identities, we say that x_1 has higher *weight* than x_2 and so on. This simply means that, while solving the system, we always prefer to write unknowns with higher weight in terms of unknowns with a lower weight.

For each numerical value of \mathbf{z} and prime p , the entries $A_{ij}(\mathbf{z})$ and $b_i(\mathbf{z})$ are evaluated and the numerical system is thus solved over finite fields. If the system is determined, for each numerical value of \mathbf{z} the solver returns a list of values for the unknowns x_j . In the more general case where there are fewer independent equations than unknowns, one can only rewrite a subset of the unknowns as linear combinations of others. This means that we identify a subset of *independent* unknowns and the complementary subset of *dependent* unknowns which are written as linear combinations of the independent ones,

$$x_i = \sum_{j \in \text{indep.}} c_{ij} x_j + c_{i0} \quad (i \in \text{dep.}). \quad (4.5)$$

Notice that the list of dependent and independent unknowns also depends on the chosen ordering (or weight) of the unknowns. The output of a linear solver is a list with the coefficients c_{ij} appearing in this solution. More specifically they are the rows of the matrix

$$\left[\{c_{ij}\}_{j \in \text{indep.}} \mid c_{i0} \right]_{i \in \text{dep.}} \quad (4.6)$$

stored in row-major order. If only the homogeneous part of the solution is needed, the elements c_{i0} are removed from the output. A node representing a linear solver is schematically depicted in fig. 3.

It often happens that only a subset of the unknowns of a system is actually needed. We therefore also have the possibility of optionally specifying a list of *needed unknowns*. When

this is provided, only the part of the solution which involves needed unknowns on the left-hand side is returned. This also allows to perform some further optimizations during the solution of the system, as we will show later.

As mentioned in section 3.2, a linear solver is an algorithm which needs a *learning step*. During this step, with a few numerical solutions of the system, the list of dependent and independent unknowns is learned. This step is also used in order to identify redundant equations, i.e. equations which are reduced to $0 = 0$ after the solution, which are thus removed from the system, improving the performance of later evaluations. Moreover, the list of dependent and independent unknowns is checked during every evaluation against the one obtained in the learning step, since accidental zeroes may change the nature of the solution of the system. If the two do not agree, the evaluation fails and the input is treated as a singular point.

It is useful to distinguish between *dense* and *sparse* systems of equations. Even if they represent the same mathematical problem, from a computational point of view they are extremely different.

Dense systems of equations are systems where most of the entries in the matrix A defined above are non-zero. For these systems, we store the n rows of the matrix

$$[A \mid b] \tag{4.7}$$

as contiguous arrays of $m + 1$ integers. We also add an $(m + 2)$ -th entry to these arrays which assigns a different numerical ID to each equation, for bookkeeping purposes. The solution is a straightforward and rather standard implementation of Gauss elimination. This distinguishes two phases. The first, also known as forward elimination, puts the system in *row echelon form*. The second, also known as back substitution, effectively solves the systems by putting it in *reduced row echelon form*. The algorithm we use for dense systems works as follows.

Forward elimination We set a counter $r = 0$, and loop over the unknowns x_k for $k = 1, \dots, m$, i.e. from higher to lower weight. At iteration k , we find the first equation E_j with $j \geq r$ where the unknown x_k is still present. If there is no such equation, we move on to the next iteration. Otherwise, we move equation E_j in position r , and we “solve” it with respect to x_k , i.e. we normalize it such that x_k has coefficient equal to 1. We thus substitute the equation in all the remaining equations below position r . We then increase r by one and proceed with the next iteration.

Back substitution We loop over the equations E_r , for $r = n, n - 1, \dots, 1$, i.e. from the one in the last position to the one in the first position. At iteration r , we find the highest weight unknown x_j appearing in equation E_r (note that this is guaranteed to have coefficient equal to one, after the forward elimination). If equation E_r does not depend on any unknown, we proceed to the next iteration. Otherwise, we substitute equation E_r , which contains the solution for x_j , in all the equations E_k with $k < r$. We then proceed with the next iteration in r .

During the learning phase, the system is solved in order to learn about the independent variables and the independent equations. The remaining equations, once the system has been reduced, will become trivial (i.e. $0 = 0$) and will, therefore, be removed. We also identify unknowns which are zero after the solution. These are then removed from the system and this allows to find, through another numerical evaluation, a smaller set of independent equations needed to solve for the non-zero unknowns. We recall that solving a dense $n \times n$ system has

$\mathcal{O}(n^3)$ complexity, hence it scales rather badly with the number of equations and unknowns, and it greatly benefits from the possibility of removing as many equations as possible.

We now discuss the reduction of *sparse* systems of equations, i.e. systems where most of the entries of the matrix A which defines it are zero. In other words, in such a system, most of the equations only depend on a relatively small subset of variables. We represent sparse systems using a sparse representation of the rows of the matrix (4.7). More specifically, for each row, we store a list of non-vanishing entries, with the number of their columns and their numerical value. These are always kept sorted by column index from the lowest to the highest, or equivalently by the weight of the corresponding unknown from the highest to the lowest. We also store additional information, namely the number of non-vanishing terms in the row, and the index of the equation corresponding to that row. When solving such systems, it is crucial to keep the equations as simple as possible at every stage of the solution. This way the complexity of the algorithm can have a much better scaling behaviour than the one which characterizes dense systems (the exact scaling strongly depends on the system itself, and it can be as good as $\mathcal{O}(n)$ in the best scenarios, and as bad as $\mathcal{O}(n^3)$ in the worst ones). For these reasons, we implement a significantly different version of Gauss elimination for sparse systems, which shares many similarities with the one illustrated in [28]. We first sort the equations by complexity, from lower to higher. The complexity of an equation is defined the same way as in ref. [28], and is determined by the following criteria, sorted by their importance,

- the highest weight unknown in the equation (higher weight means higher complexity)
- the number of unknowns appearing in the equation (a higher number means higher complexity)
- the weight of the other unknowns in the equation, from the ones with higher weight to the ones with lower weight (i.e. if two equations have the same number of unknowns, the most complex one is the one with the highest weight unknown among those that are not shared by both equations).

If all the three points above result in a tie between two equations, it means that they depend on exactly the same list of unknowns, and we say that they are equally complex, hence their relative order does not matter. Obviously, other more refined definitions of this complexity are possible, but we find that this one works extremely well for systems over finite fields, despite its simplicity. Once the equations are sorted, the algorithm for sparse systems works as follows for the forward and back substitution.

Forward elimination We create an array S whose length is equal to the number of unknowns. This will contain, at position j , the index $S(j)$ of the equation containing the solution for the unknown x_j , or a flag indicating that there is no such equation. We loop over the equations E_i for $i = 1, \dots, n$, from lower to higher complexity. If any equation is trivial (i.e. $0 = 0$), we immediately move to the next one. We find the unknowns appearing in E_i for which a solution is already found, via lookups in the array S . Among these, we select the unknown x_k such that $E_{S(k)}$ has the lowest complexity. The equation $E_{S(k)}$ is then substituted into E_i . This is repeated until all the unknowns in E_i have no solution registered in S . We then take the highest weight unknown x_h and “solve” the equation with respect to it. Once again, this means that we normalize

the equation such that the coefficient of x_h is one. We then register this solution in S by setting $S(h) = i$, and proceed with the next iteration in i .

Back substitution We remove from the system any equation which has become trivial ($0 = 0$), but otherwise, we keep them in the same order. We also update the array S to take this change into account. Let thus n_I be the number of independent equations which survived after the forward elimination. We loop again over the remaining equations E_i for $i = 1, \dots, n_I - 1$, from lower to higher complexity, excluding the last one. If a list of needed unknowns was specified, and the highest weight unknown in equation E_i is not in it, the equation is skipped. We then find the unknowns in E_i , excluding the highest weight one, for which a solution is registered in S . Among these, we pick the unknown x_k such that the equation $E_{S(k)}$ has the lowest complexity. We then substitute equation $E_{S(k)}$ in E_i . This is repeated until none of the unknowns in E_i , except the one with the highest weight, has a registered solution in S .

Similarly as before, during the learning step we identify the independent equations, removing all the other ones, and the independent unknowns. For each equation E_i , we also keep track of all the other equations which have been substituted into E_i either during the forward elimination or the back substitution. This information can optionally be used in order to further reduce the number of needed equations. Indeed, while after the learning stage the system is guaranteed to contain only independent equations, there might be a smaller subset of them which is still sufficient in order to find a solution for all the *needed unknowns*, which sometimes are a significantly smaller subset of the ones appearing in the system. This simplification is obtained, when requested, by means of the *mark and sweep* algorithm.³ After the learning stage, for each equation E_j we have a list of dependencies L_j . If $E_k \in L_j$, then E_j depends on E_k , because E_k was substituted into E_j at some point during the Gauss elimination. We identify a set R containing the so-called *roots*, which in our case are the equations containing solutions for the needed unknowns. We then “mark” all the equations in R . “Marking” is a recursive operation achieved, for any equation E_j , by setting a flag which says that E_j is needed, and then recursively marking all the equations in L_j whose flag hasn’t already been set. Finally, we “sweep”, i.e. discard all the equations which have not been marked. Notice that the mark and sweep algorithm loses some information about the system, and therefore it is only performed upon request. It is however extremely useful, e.g. when solving IBP identities, since it often reduces the size of the system by a factor even greater than the simplification achieved in the learning stage.

We also implement a dense solver algorithm called *node dense solver*, which takes the elements of the matrix in Eq. (4.7) from its input node, in row-major order, rather than from analytic formulas. In the future, we may implement a *node sparse solver* as well, which only takes the non-vanishing elements of that matrix from its input node, and uses a sparse solver for the solution.

It goes without saying that these linear solvers can also be used in order to invert matrices, using the Gauss-Jordan method. Indeed, the inverse of a $n \times n$ matrix A_{ij} is the output of a

³The mark-and-sweep method is a well known algorithm primarily used for automatic memory management (garbage collection) in order to reclaim the unused memory of a computer program. Here we use it instead to identify equations which are no longer useful (rather than allocated memory which is no longer being used), but it is based on the same mechanism.

linear solver node which solves the system

$$\sum_{j=1}^n A_{ij} x_j - t_i = 0, \quad i = 1, \dots, n, \quad (4.8)$$

with respect to the following unknowns, sorted from higher to lower weights,

$$\{x_1, \dots, x_n, t_1, \dots, t_n\}.$$

In particular, when only the homogeneous part of the solution is returned, the output of such a node will be a list with the matrix elements A_{ij}^{-1} in row-major order. Both the dense and the sparse solver can be used for this purpose, depending on the sparsity of the matrix A_{ij} . Also, notice that the matrix A_{ij} is invertible if and only if $\{x_j\}$ is the list of dependent unknowns and $\{t_j\}$ is the list of independent unknowns. This can be checked after the learning phase has completed.

4.3 Linear fit

Linear fits are another important algorithm which is often part of calculations in high energy physics. For instance, it is the main building block of integrand reduction methods (see section 7). They are also used, for instance, in order to match a result into an ansatz and to find linear relations among functions.

In general, in a linear fit, we have two types of variables, which in this section we call $\mathbf{z} = \{z_j\}$ and $\tau = \{\tau_j\}$. In particular, the \mathbf{z} variables are simply regarded as free parameters. A linear fit is thus defined by an equation of the form

$$\sum_{j=1}^m x_j(\mathbf{z}) f_j(\tau, \mathbf{z}) + f_0(\tau, \mathbf{z}) = g(\tau, \mathbf{z}) \quad (4.9)$$

where f_j and g are *known* (or otherwise *computable*) rational functions and the coefficients x_j are *unknown*. While f_j and g depend on both sets of variables, the unknown coefficients x_j can depend on the free parameters \mathbf{z} only. For each numerical value of \mathbf{z} , Eq. (4.9) is sampled for several numerical values of the variables τ . This will generate a linear system of equations for the unknowns x_j . Linear fits are thus just a special type of dense linear systems. Hence, we refer to the previous section for information about the implementation of the reduction and the output of this algorithm. In particular, each equation is associated with a particular numerical sample point for the variables $\tau = \{\tau_j\}$. In total, we use $m + n_{\text{checks}}$ sample points, where m is the number of unknowns and n_{checks} is the number of additional equations added as a further consistency check (we typically use $n_{\text{checks}} = 2$). Notice that, just like in any other linear system, redundant equations (including the additional n_{checks} ones) are eliminated after the learning phase.

In order to use this algorithm more effectively for the solution of realistic problems, and in particular integrand reduction, we made it more flexible by adding some additional features. The first one is the possibility of introducing a set of auxiliary functions $\mathbf{a} = \mathbf{a}(\tau, \mathbf{z})$ and defining several (known) functions g_j on the right-hand side, in order to rewrite Eq. (4.9) as

$$\sum_{j=0}^m x_j(\mathbf{z}) f_j(\mathbf{z}, \mathbf{a}(\tau, \mathbf{z})) + f_0(\mathbf{z}, \mathbf{a}(\tau, \mathbf{z})) = \sum_j w_j g_j(\mathbf{z}, \mathbf{a}(\tau, \mathbf{z})). \quad (4.10)$$

This is useful when the functions f_j and g_j are simpler if expressed in terms of these auxiliary variables \mathbf{a} , which do not need to be independent, and when the sum on the right-hand side is not collected under a common denominator. The value of the *weights* w_j in the previous equation depends on the inputs of the node defining the algorithm. The first input list is always the list of variables \mathbf{z} , similarly to the case of a linear system. If no other input is specified, then we simply define $w_j = 1$ for all j . If other lists of inputs are specified, besides \mathbf{z} , they are joined and interpreted as the weights w_j appearing in Eq. (4.10). This allows to define these weights numerically from the output of other nodes. As we will see in section 7, this allows, among other things, to easily implement multi-loop integrand reduction over finite fields without the need of writing any low-level code.

We provide two more usages of linear fits as nodes embedding *subgraphs* (introduced in section 3.3). The first one is used to find linear relations among the entries of the output of the subgraph G which has input variables $\{\tau, \mathbf{z}\}$. Let

$$\{f_1(\tau, \mathbf{z}), \dots, f_m(\tau, \mathbf{z})\} \quad (4.11)$$

be the output of G . The *subgraph fit* algorithm solves the linear fit problem

$$\sum_{j=1}^{m-1} x_j(\mathbf{z}) f_j(\tau, \mathbf{z}) = f_m(\tau, \mathbf{z}). \quad (4.12)$$

In particular, if \mathbf{z} is chosen to be the empty list, and $f_m = 0$, it will find vanishing linear combinations of the output of G with numerical coefficients. An interesting application of this is the attempt of simplifying the output of a graph. One can indeed estimate the complexity of each entry in the output at the price of relatively quick univariate reconstructions. A simple way of estimating the complexity is based on the total degrees of numerators and denominators, which can be found with one univariate reconstruction over one finite field, as we already explained. A more refined method would be counting the number of evaluation points needed for the reconstruction of each entry over a finite field, which can be found after the total and partial degrees have been computed and it is an upper bound on the number of non-vanishing terms in the functions. One can, of course, use any other definition or estimate for the complexity of the output functions based on other elements specific to the considered problem. Regardless of how we choose to define it, we then sort the entries by their complexity, from lower to higher, and we make sure that $f_m = 0$, e.g. by appending to the graph a Take node (this will be described in section 4.4). After solving the linear fit above for the unknowns x_j we are then able to write more complex entries of the output as linear combinations of simpler entries. When this is possible, only the independent entries need to be reconstructed.

The second subgraph application of linear fits, which we call *subgraph multi-fit*, is a generalization of the previous one. If Eq. (4.11) represents, again, the output of a graph G , the subgraph multi-fit node, which has input variables \mathbf{z} , is defined by providing a list of lists of the form

$$\{\{\sigma_{1j}\}_{j=1}^{l_1}, \{\sigma_{2j}\}_{j=1}^{l_2}, \dots\} \quad (4.13)$$

where the sublists can be of any length and σ_{ij} are integer indexes in the interval $[1, m]$. For each sublist $\{\sigma_{ij}\}_j$, the subgraph multi-fit node solves the linear fit

$$\sum_{j=1}^{l_i-1} x_{ij}(\mathbf{z}) f_{\sigma_{ij}}(\tau, \mathbf{z}) = f_{\sigma_{il_i}}(\tau, \mathbf{z}), \quad (4.14)$$

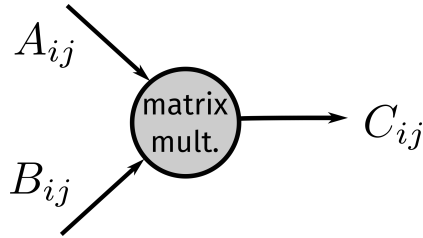


Figure 4: A node representing the matrix multiplication $C_{ij} = \sum_k A_{ik} B_{kj}$. The arrows represent lists with the matrix elements A_{ij} , B_{ij} and C_{ij} in row-major order. Their number of rows and columns is defined when the node is created.

with respect to the unknowns x_{ij} . Since this amounts to performing a number of linear fits, this node obviously has a learning phase, where independent unknowns, independent equations, and zero unknowns are detected for each one of them. Notice that all the fits can share the same evaluations of graph G , for several values of τ and fixed values of \mathbf{z} . An application of this algorithm is the case when the functional dependence of a result on the subset of variables τ (which may also be the full set of variables, if \mathbf{z} is the empty list) can be guessed a priori by building a basis of rational functions. In this case, one may create a graph G which contains both the result to be reconstructed and the elements of the function basis, and a second graph with a subgraph-fit node using G as a subgraph. This allows to reconstruct the result via a simpler functional reconstruction over the \mathbf{z} variables only, or via a numerical reconstruction if \mathbf{z} is the empty list. An example of this is given at the end of section 6.2.

4.4 Basic operations on lists and matrices

The algorithms listed in this subsection have a simple implementation and they can be thought as utilities for combining in a flexible way outputs of other numerical algorithms in the same graph. While they typically execute very quickly compared to others, they greatly enhance the possibilities of defining complex algorithms by means of the graph-based approach described in this paper. They are:

Take Takes any number of lists as input and returns a specified list of elements $\{t_1, t_2, \dots\}$ from them, where t_j can be any element of any of the input lists. The same element may also appear more than once in the output list. This is a very flexible algorithm for rearranging the output of (combinations of) other nodes. Indeed many of the list-manipulation algorithms below can also be implemented as special cases of this.

Chain Takes any number of lists as input, chains them and return them as a single list.

Slice Takes a single list as input and returns a slice (i.e. a contiguous subset of it) as output.

Matrix Multiplication Given three positive integers N_1 , N_2 and N_3 , this node takes two lists as input, interprets them as the entries of a $N_1 \times N_2$ matrix and a $N_2 \times N_3$ matrix (in row-major order) respectively, multiplies them and return the entries of the resulting $N_1 \times N_3$ matrix (still in row-major order). This node is depicted in fig. 4. Notice that, because different nodes of this type can interpret the same inputs as matrices of different sizes (as long as the total number of entries is consistent), this algorithm can also be

used to contract indexes of appropriately stored tensors, multiplying lists and scalars, and other similar operations. As an example, consider a node whose output are the entries of a rank 3 tensor T_{ABC} with dimensions N_A, N_B, N_C , and another one which represents a matrix M_{CD} with dimensions N_C and N_D . We can then perform a tensor-matrix multiplication using this node with $N_1 = N_A \times N_B$, $N_2 = N_C$ and $N_3 = N_D$. Similarly, we can multiply the tensor T_{ABC} by a scalar, the latter represented by a list of length one, by setting $N_1 = N_A \times N_B \times N_C$, $N_2 = 1$, $N_3 = 1$.

Sparse Matrix Multiplication Similar to the Matrix Multiplication above, but more suited for cases where the matrices in the input are large and sparse, so that one wants to store only their non-vanishing entries in the output of a node. This algorithm is defined by the three dimensions N_1, N_2 and N_3 as above, as well as by a list of potentially non-vanishing columns for each row of the two input matrices. The two inputs are then interpreted as lists containing only these potentially non-vanishing elements. The output of this node lists, as before, the elements of the resulting $N_1 \times N_3$ matrix, stored in a dense representation in row-major order.

Addition Takes any number of input lists of length L , and adds them element-wise.

Multiplication Takes any number of input lists of length L , and multiplies them element-wise.

Take And Add Similar to the Take algorithm above, except that it takes several lists from its inputs $\{\{t_{1j}\}_j, \{t_{2j}\}_j, \dots\}$, where each of them might have a different length. It then returns the sum of each of these sub-lists $\{\sum_j t_{1j}, \sum_j t_{2j}, \dots\}$.

Non-Zeroes This node takes one list as input and returns only the elements which are not identically zero. The node requires a learning step where the non-zero elements are identified via a few numerical evaluations (two by default). Because some algorithms have a rather sparse output (i.e. with many zeroes), it is very often useful to append this node at the end of a graph and use it as output node. This can remarkably improve memory usage during the reconstruction step. Given its benefits and its minimal impact on performance, we also recommend using such an algorithm as the output node when the sparsity of the output is not known a priori.

4.5 Laurent expansion

In physical problems, one is often interested in the leading coefficients of the Laurent expansion of a result with respect to one of its variables, which in this section we call ϵ . The most notable examples in high-energy physics are scattering amplitudes in dimensional regularization, which are expanded for small values of the dimensional regulator. Other applications can be the expansion of a result around special kinematic limits. The coefficients of this expansion are often expected to be significantly simpler than the full result. Hence, it is beneficial to be able to compute the Laurent expansion of a function without having to perform its full reconstruction first.

The Laurent expansion algorithm is another algorithm whose node embeds a subgraph. Consider a graph G representing a multi-valued $(n + 1)$ -variate rational function in the variables $\{\epsilon, \mathbf{z}\}$. The Laurent expansion node takes a list of length n as input, which represents

the variables \mathbf{z} , and returns for each output of G the coefficients of its Laurent expansion in the first variable ϵ , up to a given order in ϵ .

Without loss of generality, we only implement Laurent expansions around $\epsilon = 0$. Expansions around other points, including infinity, can be achieved by combining this node with another one implementing a change of variables, which in turn can be represented by an algorithm evaluating rational functions.

When the node is defined, we also specify the order at which we want to truncate the expansion. We can specify a different order for each entry of the output of G . This node has a learning phase, during which it performs two univariate reconstructions in ϵ of the output of G , for fixed numerical values of the variables \mathbf{z} . The first reconstruction uses Thiele’s formula, and it is used to learn the total degrees in ϵ of the numerators and the denominators of the outputs of G . Subsequent reconstructions will use the univariate system-solving strategy discussed in section 2.2. For each output of G , any overall prefactor ϵ^p , where p can be a positive or negative integer, is also detected and factored out to simplify further reconstructions (notice that, after this, we can assume the denominators to have the constant term equal to one). These prefactors also determine the starting order of the Laurent expansion, which therefore is known after the learning phase. The second reconstruction in the learning phase is simply used as a consistency check.

On each numerical evaluation, for given values of the inputs \mathbf{z} , this node performs a full univariate reconstruction in ϵ of the output of G and then computes its Laurent expansion up to the desired order. Numerical evaluations of G are cached so that they can be reused for reconstructing several entries of its output for the same values of \mathbf{z} . The coefficients of the Laurent expansions of each element are then chained together and returned.

4.6 Algorithms with no input

We finally point out that it is possible to define nodes and graphs with no input.

Nodes with no input correspond to algorithms whose output may only depend on the prime field \mathbb{Z}_p . Some notable examples are nodes implementing the solution of linear systems and linear fits (already discussed in the previous sections) in the special case where they do not depend on any list of free parameters \mathbf{z} . Another example is a node evaluating a list of rational numbers over a finite field \mathbb{Z}_p . Nodes with no input have depth zero, by definition.

A graph with no input is a graph with no input node. The nodes with the lowest depth of such a graph are nodes with no input. The output of this graph only depends on the prime field \mathbb{Z}_p used. These graphs thus represent purely numerical (and rational) algorithms and no functional reconstruction is therefore needed. For these, we perform a rational reconstruction of their output by combining Wang’s algorithm and the Chinese remainder theorem, as explained in section 2.1.

5 Reduction of scattering amplitudes

One of the most important and phenomenologically relevant applications of the methods described in this paper is the reduction of scattering amplitudes to a linear combination of master integrals or special functions. This is indeed a field which, in recent years, has received a notable boost in our technical capabilities, thanks to the usage of finite fields and functional reconstruction techniques. In particular, the results in [14, 17, 21] have been obtained using an in-development version of the framework presented here.

5.1 Integration-by-parts reduction to master integrals

Loop amplitudes are linear combinations of Feynman integrals. Consider an ℓ -loop amplitude A , or a contribution to it, with e external momenta p_1, \dots, p_e . The amplitude, in dimensional regularization, is a linear combination of integrals over the d -dimensional components of the loop momenta k_1, \dots, k_ℓ . It is convenient to write down these integrals in a standard form. For each topology T , let $\{D_{T,j}\}_{j=1}^n$ be a complete set of loop propagators, including auxiliary propagators or irreducible scalar products, such that any scalar product of the form $k_i \cdot k_j$ and $k_i \cdot p_j$ is a linear combination of them. In principle, there could also be scalar products of the form $k_i \cdot \omega_j$ where ω_j are vectors orthogonal to the external momenta p_j , but these can be integrated out in terms of denominators $D_{T,j}$ an auxiliary (see e.g. ref. [29]), hence they are not considered here. Effective methods for obtaining this representation of an amplitude are integrand reduction (discussed in section 7) and the decomposition into form factors (discussed in section 8). Hence, given a list of integers $\vec{\alpha} = (\alpha_1, \dots, \alpha_n)$, we consider Feynman integrals with the standard form

$$I_{T,\vec{\alpha}}^{(d)} = \int \left(\prod_j dk_j \right) \frac{1}{D_{T,1}^{\alpha_1} \cdots D_{T,n}^{\alpha_n}}. \quad (5.1)$$

Notice that the exponents α_j may be positive, zero, or negative.

Amplitudes may be written as linear combinations of the integrals above as

$$A = \sum_{j \in \{(T,\vec{\alpha})\}} a_j I_j, \quad (5.2)$$

where the coefficients a_j are rational functions of kinematic invariants, and possibly of the dimensional regulator $\epsilon = (4 - d)/2$. While the computation of the coefficients a_j can be highly non-trivial for high-multiplicity processes, in this section we assume them to be known. Notice that they don't need to be known analytically, but it is sufficient to have a numerical algorithm for obtaining them. As already mentioned, popular and successful examples of these algorithms are integrand reduction and the decomposition into form factors, which we will talk about in sections 7 and 8.

In general, the integrals I_j appearing in Eq. (5.2) are not all linearly independent. Indeed they satisfy linear relations such as integration-by-parts (IBP) identities, Lorentz invariance identities, symmetries, and mappings. The collection of these relations form a large and sparse system of equations satisfied by these integrals. The most well known and widely used method for generating such relations is the Laporta algorithm [30]. In this case, these identities can be easily generated using popular computer algebra systems, especially with the help of public tools (for instance, the package LITERED [31] is very useful for generating these relations in MATHEMATICA). However, any other method can be used for building this system, as long as this is provided in the form of a set of linear relations satisfied by Feynman integrals.

As explained in section 4.2, in order to properly define this system we need to introduce an ordering between the unknowns, in this case, the integrals $I_j = I_{T,\vec{\alpha}}$, by assigning a weight to them [30]. The efficiency of the linear solver, as well as the number of equations left after applying the mark-and-sweep method described in section 4.2, strongly depends on this ordering. However, there is no unique good choice of it, and any choice can be specified when

the system is defined. An example which we found has good properties and prefers integrals with no higher powers of denominators is provided in Appendix B.

By solving this large system, which we henceforth refer to as *IBP system*, we reduce the amplitude to a linear combination of a smaller set of integrals G_j , known as *master integrals* (MIs),

$$I_j = \sum_{k \in \text{MIs}} c_{jk} G_k, \quad (5.3)$$

where the coefficients c_{jk} are rational functions of the kinematic invariants and the dimensional regulator ϵ . Notice that the master integrals G_k do not need to have the form in Eq. (5.1), but they can be arbitrary combinations of integrals of that form. In general, one may have a list of preferred integrals which are defined as special linear combinations of those in Eq. (5.1) characterized by good properties, such as a simpler pole structure or a better analytic behaviour (a convenient property to have is uniform transcendental weight [32], see also section 6.2). In such cases, we add the definition of these integrals to the system of equations and we assign to them a lower weight so that they are automatically chosen as independent integrals, to the extent that this is possible, during the Gauss elimination. Another important fact to note is that the list of master integrals is determined after the learning phase of the linear solver, which only requires a few numerical evaluations.

After IBP reduction, amplitudes are written as linear combinations of master integrals

$$A = \sum_{k \in \text{MIs}} A_k G_k, \quad (5.4)$$

where the coefficients A_k , which are rational functions of the kinematic invariants and the dimensional regulator ϵ , can be obtained via a matrix multiplication between the coefficients of the unreduced amplitude in Eq. (5.2) and the ones in the IBP solutions in Eq. (5.3),

$$A_k = \sum_j a_j c_{jk}. \quad (5.5)$$

Putting these ingredients together, it is very easy to define a simple dataflow graph representing this calculation, which is depicted in fig. 5.

- The input node of the graph represents the variables $\{\epsilon, x\}$ where ϵ is the dimensional regulator and x can be any number of kinematic invariants.
- The node a_j takes as input the input node $\{\epsilon, x\}$ and evaluates the coefficients of the unreduced amplitude in Eq. (5.2). If these are known analytically this can simply be a node evaluating a list of rational functions, otherwise, it can represent something more complex, such as one of the algorithms we will discuss later.
- The IBP node is a sparse linear solver which takes as input the input node $\{\epsilon, x\}$ and returns the coefficients c_{jk} obtained by numerically solving the IBP system. Because these systems are homogeneous, we only return the homogeneous part of the solutions (the removed constant terms are zero). After the learning phase is completed, we strongly recommend running the mark-and-sweep algorithm to reduce the number of equations.
- Finally, the output node, which can be defined after the learning phase of the IBP node has been completed, is a matrix multiplication which takes as inputs the node a_j and the IBP node.

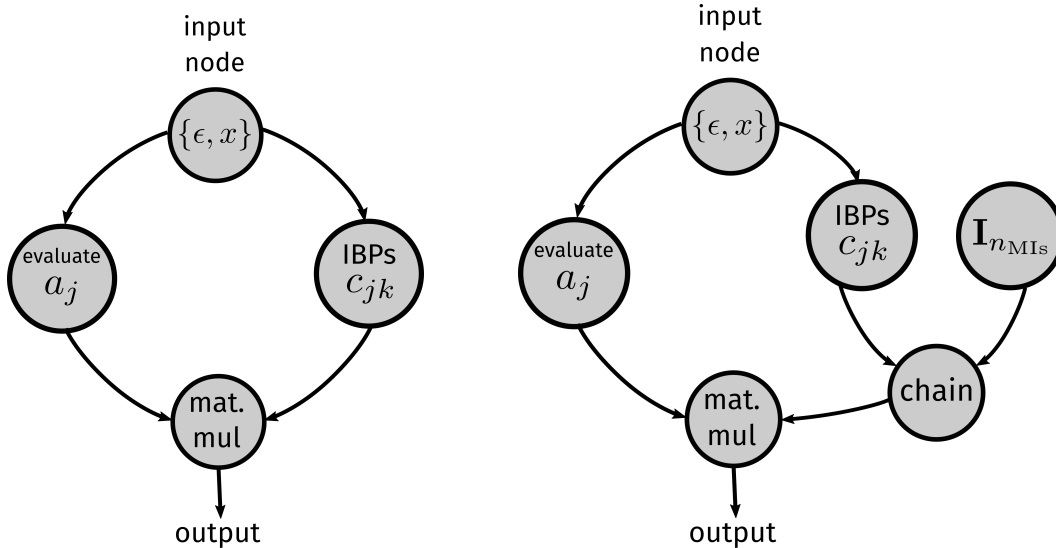


Figure 5: Two dataflow graphs representing the reduction of a scattering amplitude to master integrals. The graph on the right has two additional nodes chaining to the coefficients of the IBP solutions an identity matrix, which represents the (trivial) reduction of the master integrals themselves. These nodes are needed when the masters can also appear on the r.h.s. of the unreduced amplitude in Eq. (5.2).

The graph we just described, which is depicted on the left of fig. 5, ignores a technical subtlety. The reduction coefficients c_{jk} returned by the IBP node express the non-master integrals in terms of master integrals. However, depending on our choice of masters, the master integrals themselves may also appear on the r.h.s. of the unreduced amplitude in Eq. (5.2). This creates a mismatch which does not allow to properly define the final matrix multiplication. More explicitly, if n_{MIs} is the number of master integrals, and $n_{\text{non-MIs}}$ is the number of non-master integrals appearing in Eq. (5.2), then the IBP node returns a $n_{\text{non-MIs}} \times n_{\text{MIs}}$ matrix. However, if the n_{MIs} masters also appear on the r.h.s. of Eq. (5.2), then the output of the a_j node has length $n_{\text{non-MIs}} + n_{\text{MIs}}$, which makes it incompatible with the IBP solution matrix it should be multiplied with. This can, however, be easily fixed by defining an additional node representing the reduction of the master integrals to themselves, which is trivially given by the $n_{\text{MIs}} \times n_{\text{MIs}}$ identity matrix $\mathbf{I}_{n_{\text{MIs}}}$ (this is a node with no input, which evaluates a list of rational numbers, see also section 4.6). After this is chained (see section 4.4) to the output of the IBP node, we obtain a $(n_{\text{non-MIs}} + n_{\text{MIs}}) \times n_{\text{MIs}}$ matrix containing the reduction to master integrals of all the $n_{\text{non-MIs}} + n_{\text{MIs}}$ Feynman integrals in Eq. (5.2). Hence the final matrix multiplication is well defined. This graph is depicted on the right of fig. 5. Notice that these two extra nodes are not necessary when all the master integrals have been separately defined and don't appear in our representation of the unreduced amplitude, because in this case the output of the a_j node has length $n_{\text{non-MIs}}$ and can be directly multiplied with the matrix computed by the IBP node.

The dataflow graph we just described computes the coefficients of the reduction of an amplitude to master integrals. By evaluating this graph several times, one can thus reconstruct the analytic expressions of these coefficients, without the need of deriving large and complex IBP tables. This represents a major advantage, since IBP tables for complex processes can be

extremely large, significantly more complex than the final result for the reduced amplitude, hard to compute, and also hard to use – since they require to apply a huge list of complex substitutions to the unreduced amplitude. On the other hand, using the approach described here, IBP tables are always computed numerically, and only the final result is reconstructed analytically. Hence, by building a very simple dataflow graph consisting of only a few nodes, we are able to sidestep the bottleneck of computing and using large, analytic IBP tables. This approach has already allowed (e.g. in ref.s [14, 21]) to perform reductions in cases where the IBP tables are known to be too large and complex to be computed and used with reasonable computing resources.

5.2 Reduction to special functions and Laurent expansion in ϵ

The expansion in the dimensional regulator ϵ of the master integrals can often be computed in terms of special functions, such as multiple polylogarithms or their elliptic generalization. When this is possible, the result for the ϵ expansion of a scattering amplitude might be significantly simpler than the one in terms of master integrals. For the sake of argument, we assume to be interested in the poles and the finite part of the amplitude, but everything we are going to discuss can be easily adapted to different requirements.

Let $\{f_k = f_k(x)\}$ be a complete list of special functions (which may also include numerical constants) such that every master integral G_j , expanded up to its finite part, can be expressed in terms of these as

$$G_j = \sum_{jk} g_{jk}(\epsilon, x) f_k + \mathcal{O}(\epsilon), \quad (5.6)$$

where g_{jk} are rational functions in ϵ and x (typically, they will be a Laurent polynomial in ϵ , but this is not important for the discussion). Recalling Eq. (5.4), we can thus write the amplitude in terms of these functions as

$$A = \sum_k u_k(\epsilon, x) f_k + \mathcal{O}(\epsilon), \quad (5.7)$$

where the rational functions u_k are defined as

$$u_k(\epsilon, x) = \sum_j A_j(\epsilon, x) g_{jk}(\epsilon, x). \quad (5.8)$$

We are interested in the expansion in ϵ of the coefficients u_k , i.e. in the coefficients $u_k^{(j)} = u_k^{(j)}(x)$ such that

$$u_k(\epsilon, x) = \sum_{j=-p}^0 u_k^{(j)}(x) \epsilon^j + \mathcal{O}(\epsilon), \quad (5.9)$$

where p is such that the leading pole of the amplitude is proportional to ϵ^{-p} .

Computing the coefficients $u_k^{(j)}(x)$ in our framework is straightforward. We start from the dataflow graph described in section 5.1, which computes the coefficients A_j of the master integrals. We first extend this graph in order to get the unexpanded coefficients $u_k(\epsilon, x)$. This is simply done by adding a node g_{jk} , which evaluates the rational functions $g_{jk}(\epsilon, x)$ defined in Eq. (5.6), and a matrix multiplication node between the node A_j (which was the output node in the previous case) and g_{jk} , as one can see from Eq. (5.8). Let us call this dataflow

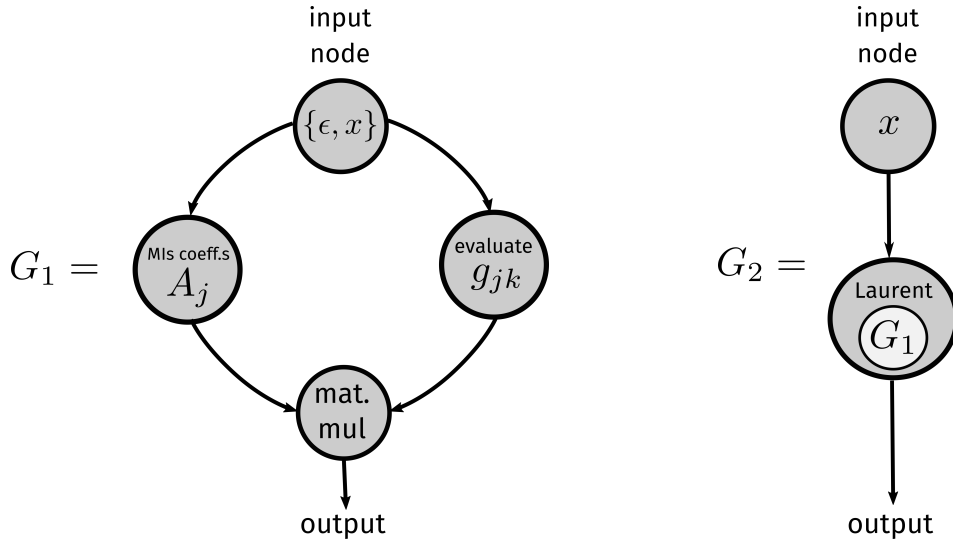


Figure 6: Two graphs which, combined, compute the ϵ expansion of the coefficients of scattering amplitudes in terms of special functions. In the first graph G_1 , A_j represents the calculation of the coefficients of the master integrals presented in section 5.1 and fig. 5. The graph G_2 then takes the graph G_1 as subgraph in one of its nodes, which computes its Laurent expansion in ϵ .

graph G_1 . We then create a new graph G_2 with input variables x . Inside the latter, we create a Laurent expansion node, which takes as its subgraph G_1 . The output of this node will be the coefficients $u_k^{(j)}$ of the Laurent expansion in Eq. (5.9). This is depicted in fig. 6.

Because the coefficients $u_k^{(j)}(x)$ might not be all linearly independent, we also recommend running the *subgraph fit* algorithm described in section 4.3 in order to find linear relations between them. In particular, this can be used to rewrite the most complex coefficients as linear combinations of simpler ones, yielding thus a more compact form of the result, which is also easier to reconstruct.

We finally point out that one can further elaborate the graph G_1 in order to include *renormalization*, *subtraction* of infrared poles, and more. This is done by rewriting these subtractions, which are typically known analytically since they depend on lower-loop results, in terms of the same list of functions $\{f_k\}$ as the amplitude. After doing so, the coefficients of the subtraction terms multiplying the functions f_k are added to the graph as nodes evaluating rational functions and summed to the output using the Addition node described in section 4.4. This may thus simplify the output of the Laurent expansion computed in the graph G_2 , which will, therefore, be easier to reconstruct.

It goes without saying that, even if we focused on scattering amplitudes, the same strategy can be applied to other objects in quantum field theory which have similar properties, such as correlation functions and form factors.

6 Differential equations for master integrals

Integration-by-parts identities are not only useful to reduce amplitudes to linear combinations of a minimal set of independent master integrals, but they are also helpful for the calculation

of the master integrals themselves via the method of differential equations [33, 34]. Indeed the master integrals G_j satisfy systems of coupled partial differential equations with respect to the invariants x ,

$$\frac{\partial}{\partial x} G_j = \sum A_{jk}^{(x)}(\epsilon, x) G_k. \quad (6.1)$$

Solving these systems of differential equations is one of the most effective and successful methods for computing the master integrals.

6.1 Reconstructing differential equations

The differential equation matrices can be easily computed within our framework, using a strategy which is completely analogous to the one described in section 5.1 for the reduction of scattering amplitudes to master integrals.

We first determine the master integrals by solving the IBP system numerically over finite fields. For this, we need to specify a list of *needed integrals*, i.e. a list of needed unknowns for which the system solver is asked to provide a solution since in general one cannot reduce to master integrals all the integrals appearing in an IBP system. We then make a conservative choice which is likely to be a superset of all the integrals which need to be reduced for computing the differential equations.

Then, the derivatives of master integrals with respect to kinematic invariants can be easily computed analytically,

$$\frac{\partial}{\partial x} G_j = \sum_{k \in (T, \bar{\alpha})} a_{jk}^{(x)} I_k, \quad (6.2)$$

where the integrals I_j have the standard form defined in Eq. (5.1), and $a_{jk}^{(x)}$ are rational functions of the invariants x . At this stage, we may reset the list of needed unknowns of the IBP system to include only the ones appearing on the r.h.s. of Eq. (6.2). After that, we also strongly suggest running the mark-and-sweep algorithm for removing unneeded equations.

By solving the IBP system, we reduce the integrals I_j to master integrals. This defines the coefficients c_{jk} of the reduction, as in Eq. (5.3). The differential equation matrices $A_{jk}^{(x)}$ are thus obtained via the matrix multiplication

$$A_{jk}^{(x)} = \sum_l a_{jl}^{(x)} c_{lk}. \quad (6.3)$$

A dataflow graph representing this calculation can, therefore, be almost identical to the one described in section 5.1, and it is depicted on the left side of fig. 7. In particular, it has an input node representing the variables $\{\epsilon, x\}$, a node evaluating the rational functions $a_{ij}^{(x)}$ appearing in the unreduced derivatives of Eq. (6.2), a node with the IBP system, and an output node with the final matrix multiplication in Eq. (6.3). Similarly to the case of the amplitudes, if the master integrals are chosen such that they can also appear on the r.h.s. of the unreduced derivatives in Eq. (6.2), then we also add an identity matrix node, and a node chaining this to the IBP node (see section 5.1 and fig. 5 for more details).

By defining this graph, we can reconstruct the differential equations of the master integrals directly, without the need of computing IBP tables analytically, similarly to the case of the reduction of amplitudes. This usually yields a substantial simplification of the calculation.

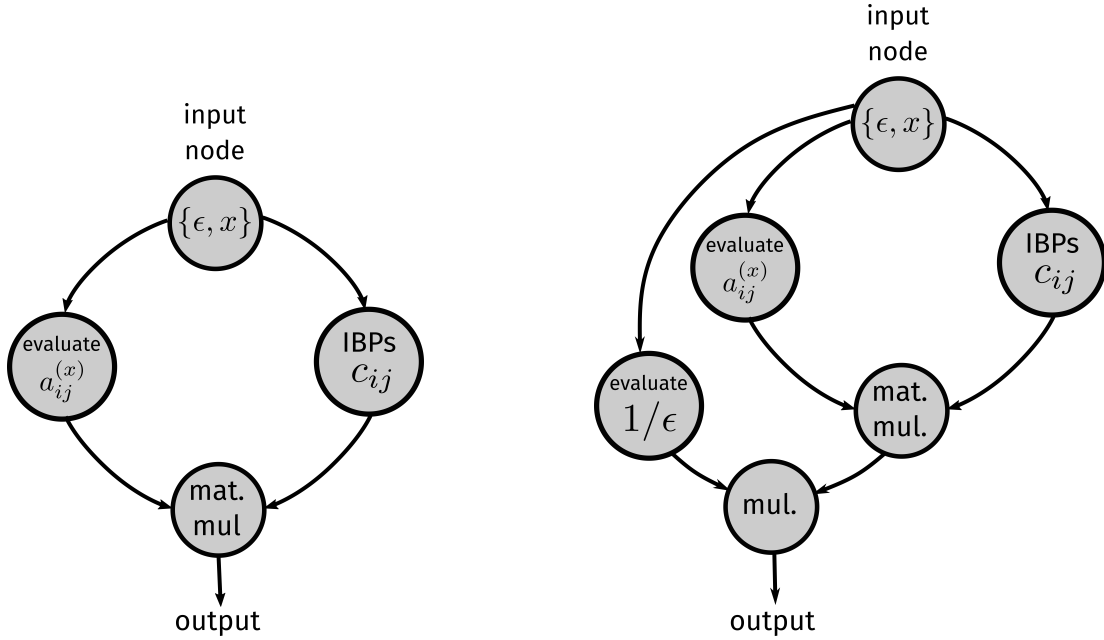


Figure 7: On the left, a dataflow graph representing the calculation of differential equations satisfied by master integrals. It is similar to the one depicted in fig. 5 for the reduction of amplitudes to master integrals. On the right, a dataflow graph computing the differential equation matrices divided by ϵ . As explained in section 6.2 we can verify the ϵ -form of the differential equations by checking numerically that the output of the latter graph does not depend on ϵ .

6.2 Differential equations in ϵ -form

It has been observed in ref. [32] that the differential equation method becomes more powerful and effective if the master integrals are chosen such that they are *pure functions of uniform transcendent weight*, henceforth *UT functions* for brevity (we refer to ref. [32] for a definition). Remarkably, as pointed out in ref. [32], one can build a list of integrals having this property without doing any reduction at all, by using some effective rules or by analyzing the leading singularities of Feynman integrals. A systematic algorithm which implements this analysis of leading singularities was developed and described in [35], and recently extended in ref. [36]. Once a (possibly over-complete) list of UT integrals has been found, their definitions can be added as additional equations to the IBP system. By assigning a lower weight to these integrals, they will be automatically chosen as preferred master integrals by the system solver.

If $\{G_k\}$ represents a basis of UT master integrals, the differential equation matrices take the form [32]

$$A_{ij}^{(x)}(\epsilon, x) = \epsilon A_{ij}^{(x)}(x), \quad (6.4)$$

i.e. their ϵ dependence is simply an ϵ prefactor. This greatly simplifies the process of solving the system perturbatively in ϵ . When this happens, the system of differential equations is said to be in ϵ -form or in canonical form.

If a list of UT candidates is known, as we said, we may add their definition to the IBP system, and then we divide the final result for the matrices by ϵ . This is done by modifying the dataflow graph defined before, with the addition of a node which evaluates the rational

function $1/\epsilon$, and a new output node which multiplies the $1/\epsilon$ node with the older output node. As mentioned in section 4.4, the multiplication can be accomplished using a matrix multiplication node, which interprets $1/\epsilon$ as a 1×1 matrix and its second input node as a matrix with only one row. This modified graph is depicted on the right side of fig. 7. Once the graph is defined, we can evaluate it numerically for several values of ϵ while keeping x fixed, in order to check that the system is indeed in ϵ -form.

Differential systems in ϵ -form for UT integrals are typically much easier to reconstruct since they have a particularly simple functional structure. Hence they benefit even more from the functional reconstruction methods described in this paper, which allow to reconstruct this result directly without dealing with the significantly more complex analytic intermediate expressions one would have in a traditional calculation.

A large class of Feynman integrals can be written as linear combinations of iterated integrals of the form (using the notation in [37])

$$\int d \log w_1 \circ d \log w_2 \circ \dots \circ d \log w_n \quad (6.5)$$

where the $d \log$ arguments w_k are commonly called *letters*. A complete set of letters is called *alphabet*. While the alphabet of a multi-loop topology is often inferred from the differential equations for the master integrals, there are some cases where this can instead be guessed a priori. In such cases, finding differential equations for UT master integrals can be even simpler, since the calculation can be reduced to a numerical linear fit [38]. Indeed, it is well known that differential equations matrices for UT master integrals, aside from their ϵ prefactor, are expected to be linear combinations of first derivatives of logarithms of letters, with rational numerical coefficients. More explicitly, if $W = \{w_1, w_2, \dots\}$, with $w_k = w_k(x)$, is the alphabet of a topology, the differential equation matrices for a set of UT master integrals take the form

$$A_{ij}^{(x)}(x) = \sum_k \frac{\partial \log(w_k)}{\partial x} C_{ij}^{(x,k)}, \quad (6.6)$$

where $C_{ij}^{(x,k)}$ are rational numbers. Hence, rather than employing multivariate functional reconstruction methods, in this case, we can compute the differential equation matrices just with a linear fit. For this purpose, we can apply the *subgraph multi-fit* algorithm described in section 4.3. More explicitly, we create a graph G_1 whose output contains both the derivatives $\partial \log w_k / \partial x$ of the letters and the (non-vanishing) matrix elements $A_{ij}^{(x)}$. We then build a second graph G_2 , with a subgraph multi-fit node containing G_1 , which performs a fit of each matrix element with respect to the basis of functions $\{\partial \log w_k / \partial x\}$, as described in section 4.3. Notice that G_2 has no input node, and therefore we run a numerical reconstruction of its output over \mathbb{Q} using Wang's algorithm and the Chinese remainder theorem, as already explained in section 4.6.

6.3 Differential equations with square roots

In our discussion of differential equations for UT integrals, we have so far neglected the potential issue of the presence of square roots in their definition. Indeed, there are cases where, in order to define UT integrals, one needs to take rational linear combinations of integrals of the form of Eq. (5.1) and multiply them by a prefactor equal to the square root of a rational function of the invariants x . Even in cases where these square roots may

be removed via a suitable change of variables, one may still wish to compute differential equations in terms of the original kinematic invariants, at least as a first step. While square roots may be accommodated in our framework by considering finite fields which are more general than \mathbb{Z}_p , we would like to point out in this section that this is not necessary for computing differential equations.

Let us rewrite the master integrals G_j as

$$G_j = R_j G_j^{\text{r.f.}}, \quad (6.7)$$

where R_j is either equal to one or to the square root of a rational function of the invariants x , and $\{G_j^{\text{r.f.}}\}$ are a set of root-free master integrals, which can be written as rational linear combinations of standard Feynman integrals of the form of Eq. (5.1). We first observe that the quantity

$$\frac{1}{R_j} \frac{\partial}{\partial x} G_j = \left(\frac{1}{R_j} \frac{\partial R_j}{\partial x} \right) G_j^{\text{r.f.}} + \frac{\partial}{\partial x} G_j^{\text{r.f.}}, \quad (6.8)$$

which can be easily computed analytically, is also a rational combination of standard Feynman integrals. This is indeed manifest on the r.h.s. of the equation, since if R is the square root of a rational function then R'/R is rational. This implies that, via IBP identities, we can reduce the root-free quantity in Eq. (6.8) to the root-free master integrals and obtain

$$\frac{1}{R_j} \frac{\partial}{\partial x} G_j = \sum_k \tilde{A}_{jk}^{(x)} G_k^{\text{r.f.}}, \quad (6.9)$$

where the matrix $\tilde{A}_{jk}^{(x)}$ is also rational since the IBP reduction itself cannot introduce any non-rational factor. One can finally show that the matrix $\tilde{A}_{jk}^{(x)}$ is related to the differential equation matrix $A_{jk}^{(x)}$ we wish to compute by

$$A_{jk}^{(x)} = \frac{R_j}{R_k} \tilde{A}_{jk}^{(x)}, \quad (6.10)$$

i.e. simply by rescaling each matrix element by a prefactor. We can, therefore, apply the methods described above to the quantity in Eq. (6.8) (rather than to the simple derivatives of the master integrals), use it to reconstruct the rational matrix $\tilde{A}_{jk}^{(x)}$, and finally recover $A_{jk}^{(x)}$ by introducing the appropriate prefactors. Notice also that $A_{jk}^{(x)}$ is in ϵ -form if and only if $\tilde{A}_{jk}^{(x)}$ is in ϵ -form.

7 Integrand reduction

In section 5, we explained how to compute the reduction of a scattering amplitude, either to a linear combination of master integrals or to a combination of special functions expanded in the dimensional regulator. One of the ingredients of the algorithm discussed there was a representation of the unreduced amplitude (cfr. with Eq. (5.2)) as a linear combination of Feynman integrals cast in a standard form, such as the one in Eq. (5.1). In particular, within the FINITEFLOW framework, we need a numerical algorithm capable of computing the coefficients a_j of such a linear combination. This is trivial if an analytic expression is known for the a_j . However, this is not always the case. Indeed, for complex processes, casting the

amplitude in such a form is a very challenging problem. In this section, we discuss *integrand reduction* methods [3–8, 29], which are an efficient way of obtaining this representation of the amplitude and are suitable for complex processes.

7.1 Integrand reduction via linear fits

Amplitudes are linear combinations of integrals of the form

$$A = \int \left(\prod_j dk_j \right) \frac{\mathcal{N}(k_1, \dots, k_\ell)}{D_1^{\alpha_1} \dots D_n^{\alpha_n}}, \quad \alpha_j > 0, \quad (7.1)$$

where \mathcal{N} is a polynomial numerator in the loop components, and D_j are denominators of loop propagators. For simplicity, we consider only one topology, identified by a set of loop denominators, but we understand that the approach discussed here should be applied to all the topologies contributing to the amplitude we wish to compute.

Integrand reduction methods rewrite the integrand as a linear combination of functions belonging to an *integrand basis*

$$\frac{\mathcal{N}(k_j)}{D_1^{\alpha_1} \dots D_n^{\alpha_n}} = \sum_{\beta_j | 0 \leq \beta_j \leq \alpha_j} \frac{\Delta_{\beta_1 \dots \beta_n}}{D_1^{\beta_1} \dots D_n^{\beta_n}}, \quad (7.2)$$

where $\Delta_{\vec{\beta}} \equiv \Delta_{\beta_1 \dots \beta_n}$ has the form

$$\Delta_{\vec{\beta}} = \sum_j c_{\vec{\beta}, j} m_{\vec{\beta}, j}(k_1, \dots, k_\ell). \quad (7.3)$$

In the previous equations, the functions $m_{\vec{\beta}, j}$ are a complete set of *irreducible numerators*, i.e. numerators which, at the integrand level, cannot be written in terms of the loop propagators they are sitting on. In other words, the terms

$$\frac{m_{\vec{\beta}, j}(k_1, \dots, k_\ell)}{D_1^{\beta_1} \dots D_n^{\beta_n}} \quad \text{with } 0 \leq \beta_1 \leq \alpha_1, \dots, 0 \leq \beta_n \leq \alpha_n, \quad (7.4)$$

must form a complete basis of rational functions in the loop components, for the loop integrand we are interested in. The coefficients $c_{\vec{\beta}, j}$, which do not depend on the loop momenta but only on the kinematic invariants, are unknowns which parametrize an integrand in terms of the chosen basis. The functions $\Delta_{\vec{\beta}}$, also known in the literature as *residues* or *on-shell integrands*, collect the elements of the integrand basis which share the same loop-denominator structure. The integrand basis can be chosen a priori solely based on the loop topology, and independently of the process or the particle content of the loop diagrams (see below for a few examples). The parametric coefficients $c_{\vec{\beta}, j}$ in Eq. (7.3) are instead process dependent and represent the unknowns of this representation.

Once an integrand basis has been chosen, the unknown coefficients $c_{\vec{\beta}, j}$ can be determined via a *linear fit*. For this purpose, we can use the algorithm described in section 4.3, using kinematic invariants as the free parameters \mathbf{z} , loop variables as the additional set of variables τ , and $c_{\vec{\beta}, j}$ as the unknowns of the system. In particular, in a dimensional regularization

scheme where the external states are four-dimensional (such as the t'Hooft-Veltman [39] and Four-Dimensional-Helicity [40] schemes), the integrand depends on

$$4\ell + \frac{\ell(\ell + 1)}{2}$$

loop variables. These can be chosen, for instance, as the four-dimensional components of the loop momenta with respect to a basis of four-dimensional vectors, plus the independent scalar products between the extra-dimensional projections of the loop momenta

$$\mu_{ij} = -k_i^{[-2\epsilon]} \cdot k_j^{[-2\epsilon]}. \quad (7.5)$$

While performing a global fit of all the coefficients at the same time is theoretically possible, in practice it is extremely inefficient and impractical, because it involves solving a dense system of linear equations of the same size as the number of the unknown coefficients. One can however greatly simplify the problem by splitting it into several smaller linear fits, using the so-call *fit-on-the-cut* approach [3]. This consists of evaluating the integrand on *multiple cuts*, i.e. values of the loop momenta such that a subset of loop propagators vanish (we also understand that vanishing denominators should be removed from the integrand when applying a cut). On each cut, we also have fewer independent loop variables τ , namely those which are not fixed by the cut conditions. This method is best used in a top-down approach. We first cut (i.e. set to zero) as many propagators as possible, and use linear fits on maximal cuts for determining a first set of coefficients. We then proceed with linear fits on cuts involving fewer and fewer propagators. When performing a fit on a multiple cut, on-shell integrands which have already been fixed on previous cuts are first subtracted from the integrand. These subtractions are sometimes referred to as *subtractions at the integrand level*. If an integrand has all denominator powers α_j equal to one, with this approach we determine the coefficients of one and only one on-shell integrand $\Delta_{\vec{\beta}}$ on each cut. If higher powers of propagators are present, more than one off-shell integrand must be determined at the same time on some cuts, but this doesn't qualitatively change the algorithm for the linear fit (this point is discussed more in detail in ref.s [41, 42]).

Subtractions at the integrand level can be implemented using the linear fit algorithm described in Eq. (4.10). In particular, we define a dataflow graph where each multiple cut corresponds to a different node, whose output is the list of coefficients $c_{\vec{\beta}, j}$ determined by a linear fit. Each node takes as input, besides the kinematic variables \mathbf{z} , the output of all the higher-point cuts with non-vanishing subtractions on the current cut. The coefficients returned by the input nodes will be used as weights w_j (cfr. with Eq. (4.10)) for the subtractions, while the integrand will typically have weight one. Notice that the linear fit described in Eq. (4.10) also allows to define a set of auxiliary functions, in terms of which we can express both the integrand and the integrand basis. This is very convenient since it allows to express these objects in terms of scalar products, spinor chains, or other auxiliary functions which may yield a simple representation. Hence, we only have to explicitly substitute the cut solutions inside these functions, which are then evaluated numerically. In particular, we don't need to substitute the cut solutions inside the full integrand or the full set of integrand basis elements appearing in the subtraction terms, which may yield complicated expressions in some cases.

We also note that, when using the loop variables described above, finding a rational parametrization of the cut solutions is a simple problem of linear algebra. As already explained

in [29] one can proceed by splitting the cut denominators into categories, such that denominators in the same category depend on the same subset of loop momenta. For each category, we choose a representative, and we take differences between all the other denominators and this representative. This gives a linear system of equations for the four-dimensional components of the loop momenta which live in the space spanned by the external legs. Next, we complete this solution by setting to zero the representatives of each category. This gives a system of equations which is linear in the variables μ_{ij} . Notice that this is only true when we work in d dimensions.

If neither the integrand nor the integrand basis depends on the dimensional regulator ϵ , it is convenient to embed the integrand reduction nodes in a *memoized subgraph*, as described at the end of section 3.3. During the Laurent expansion, this avoids repeating the integrand reduction for several values of ϵ and fixed values of the kinematic invariants. If the integrand has a polynomial dependence on ϵ , as it happens for amplitudes in the t'Hooft-Veltman regularization scheme, we can still implement this improvement by using several memoized subgraphs, i.e. one for each power of ϵ in the numerator.

The algorithm we described allows to define a dataflow graph implementing a full multi-loop integrand reduction over finite fields, starting from a known integrand and an integrand basis. This is particularly convenient when using FINITEFLOW from a computer algebra system. The output of all these nodes can then be collected, using either a Chain or a Take algorithm (see section 4.4), and used as input for subsequent stages of the reduction, such as IBP reduction, and the decomposition in terms of known special functions, as described in section 5. In our experience, this strategy is very efficient, even on complex multi-loop integrands, especially if compared with the more time-consuming IBP reduction step.

It is also worth mentioning that integrand reduction is often used in combination with *generalized unitarity* [4, 9–12]. On multiple cuts the integrand factorizes as a product of tree-level amplitudes, which in turn may be evaluated efficiently, over a numerical field, using Berends-Giele recursion [43]. We refer to ref. [2] for a complete description of an implementation of generalized unitarity over finite fields. It should be noted that, while generalized unitarity is an extremely powerful method which can substantially reduce the complexity of the calculation, it also has some limitations. For instance, one needs to find rational finite-dimensional parametrizations for the internal states of the loop on the cut solutions, which is not always easy. Moreover, in its current state, it cannot be easily applied to processes with massive internal propagators. These difficulties and limitations are not present when applying integrand reduction to a diagrammatic representation of the amplitude.

7.2 Choice of an integrand basis

It is worth making some observations on possible choices for an integrand basis. In the one-loop case, one can choose a basis which yields a linear combination of known integrals [3, 4]. With this choice, IBP reduction is not needed. At higher loops, this is not the case, and one should therefore take into account that the elements of an integrand basis should be later reduced via IBP identities.

A particularly simple but effective choice, especially at the multi-loop level, consists of writing any on-shell integrand $\Delta_{\vec{\beta}}$ in terms of the denominators and auxiliaries $\{D_{T,j}\}$ of its parent topology T such that $\beta_j = 0$, i.e. excluding the ones that $\Delta_{\vec{\beta}}$ is sitting on. In processes with fewer than five external legs, one must also include scalar products of the form $k_i \cdot \omega_j$ where $\{\omega_j\}$ are a complete set of four-dimensional vectors orthogonal to all the

external momenta p_1, \dots, p_e . Hence, $\Delta_{\vec{\beta}}$ can be parametrized as the most general polynomial in this set of variables, whose total degree is compatible with the theory. For instance, a renormalizable theory allows at most one power of loop momenta per vertex, in the sub-topology defined by the denominators of $\Delta_{\vec{\beta}}$. After integrand reduction, the scalar products of the form $k_i \cdot \omega_j$ can be integrated out in terms of denominators and auxiliaries $D_{T,j}$. As explained e.g. in [29], this can be easily done via a tensor decomposition in the $(d - e + 1)$ -dimensional subspace orthogonal to the e external momenta. Notice that this is very simple even for complex processes since it only involves the orthogonal projection of the metric tensor $g_{[d-e+1]}^{\mu\nu}$ and no external momentum. Alternatively, one can achieve the same result via an angular loop integration over the orthogonal space, which can be made even simpler using Gegenbauer polynomials [29]. This choice of integrand basis directly yields, after orthogonal integration, a linear combination of integrals which are suitable for applying standard IBP identities. Given also its simplicity, it is a recommended choice in most cases.

Other choices can be made for the sake of having either a simpler integrand representation or a larger set of elements of the integrand basis which integrate to zero. One can, for instance, choose to replace monomials in an on-shell integrand with monomials involving also the extra-dimensional scalar products μ_{ij} . Because monomials with μ_{ij} can be rewritten as linear combinations of the other ones, one can easily obtain a system of equations relating these two types of monomials. By solving this system, assigning a lower weight to monomials involving μ_{ij} , one can maximize the presence of integrands which vanish in the four-dimensional limit. Since we are only interested in a list of independent monomials, it is sufficient to solve the system numerically (possibly over finite fields). This is heuristically found to yield simpler integrand representations. However, it also makes IBP reduction harder to use, since integrands with μ_{ij} then need to be converted to the ones in a standard form. If only the finite part of the amplitude is needed, one may however choose some integrands involving μ_{ij} which are $\mathcal{O}(\epsilon)$ after integration and then drop them before the IBP reduction step. This may result in notable simplifications. As an example, at one loop, no on-shell integrand with more than four denominators contributes to the finite part of an amplitude, if μ_{11} is chosen to be the numerator of the five-denominator integrands in the integrand basis.

Another popular choice is the usage of scalar products involving momenta which, for an on-shell integrand $\Delta_{\vec{\beta}}$, are orthogonal to the external momenta of the topology defined by its own denominators (as opposed to the ones of the parent topology). One can indeed build suitable combinations of these scalar products which vanish upon integration. Their coefficients can then be dropped after the integrand reduction.

Another very successful strategy is the usage, for each on-shell integrand $\Delta_{\vec{\beta}}$, of a complete set of *surface terms*, i.e. terms which vanish upon integration and are compatible with multiple cuts [44–47]. These are chosen to be an independent set of IBP equations without higher powers of denominators. These define suitable polynomial numerators for $\Delta_{\vec{\beta}}$ which vanish upon integration. When this approach is used, IBP reduction is embedded in the integrand reduction and therefore it is not needed as a separate step. A possible disadvantage is that it makes the integrand reduction more complicated, since these surface terms are typically more complex than the elements of other integrand bases, and they introduce a dependence on the dimensional regulator which is otherwise not present in the integrand reduction stage. Another disadvantage is that, in the form it is usually formulated, this strategy can yield incomplete reductions for some processes.⁴

⁴Indeed, one can see that, in the references above, these surface terms are effectively chosen to be linear

We finally point out that, if there is no one-to-one correspondence between elements of the integrand basis and Feynman integrals to be reduced via IBPs, one needs to convert between the two. This step may also include the transverse integration, if needed. The conversion, as in many other cases, can be implemented via a matrix multiplication. For this purpose, we recommend using either the Take And Add algorithm or the Sparse Matrix Multiplication algorithm described in section 4.4.

7.3 Writing the integrand

When using integrand reduction together with Feynman diagrams, one would typically provide the integrands in Eq. (7.1) analytically. Even if several methods exist for generating integrands numerically at one loop, with the notable exception of generalized unitarity (which is however not based on Feynman diagrams and has the limitations mentioned above) they have not been generalized to higher loops. When integrands are provided in some analytic form, they will also depend on external polarization vectors, spinor chains, and possibly other objects describing the external states. On one hand, this means that we need to provide a rational parametrization for these objects. On the other, we may use the algorithms described above in order to keep these rational expressions as compact as possible. This is done by performing the substitutions which would yield complex expressions only numerically over finite fields.

A rational parametrization for four-dimensional spinors, polarization vectors, external momenta, as well as higher-spin polarization states, can be obtained, in terms of a minimal set of invariants, by means of the so-called *momentum twistor parametrization* [48–50]. The independent kinematic invariants are called in this case *momentum twistor variables*. A comprehensive description of the usage of this parametrization for describing external states in the context of numerical calculations over finite fields is given in ref. [2] and will not be repeated here.

In amplitudes with only scalars and spin-one external particles, the only additional loop-dependent objects appearing in the integrand, besides the loop denominators and auxiliaries, are scalar products between loop momenta and polarization vectors. If external fermions are present, one also has spinor chains involving loop momenta. These can be dealt with by splitting the loop momenta in a four-dimensional and a (-2ϵ) -dimensional part

$$k_j^\mu = k_j^{[4]\mu} + k_j^{[-2\epsilon]\mu}, \quad (7.6)$$

and performing the t'Hooft algebra on the extra-dimensional components in order to explicitly convert all the dependence on $k_j^{[-2\epsilon]}$ into the extra-dimensional scalar products μ_{ij} defined in Eq. (7.5).

The four-dimensional part of the loop momenta is often decomposed into a four-dimensional basis. Given a generic loop momentum k and three massless momenta p_1, p_2, p_3 , we can use the decomposition, in spinor notation,

$$k^{[4]\mu} = y_1 p_1^\mu + y_2 p_2^\mu + y_3 \frac{\langle 23 \rangle \langle 1 \sigma^\mu 2 \rangle}{\langle 13 \rangle} + y_4 \frac{\langle 13 \rangle \langle 2 \sigma^\mu 1 \rangle}{\langle 23 \rangle}. \quad (7.7)$$

combinations of IBP identities whose seed integrals do not have higher powers of denominators than the ones in the diagrams which need to be reduced. Hence, whenever identities using seed integrals with higher powers of denominators, or seed integrals with more propagators, are needed to fully reduce a given sector, the method above will not yield a complete reduction to a minimal basis of master integrals. Examples where we explicitly checked that additional seed integrals are needed are several two-loop topologies involving massive internal propagators (e.g. topologies for amplitudes with two fermion pairs having different masses), and some massless four-loop topologies (including most of those reduced in ref. [17]).

The massless momenta can be chosen depending on the cut, but it is also possible, and often easier, to define a global basis of momenta and therefore use the same set of loop variables y_j and μ_{ij} everywhere. If there aren't enough massless external legs, one may use massless projections of massive ones or arbitrary massless reference vectors. In some cases, it is convenient to make the substitution in Eq. (7.7) directly in the analytic integrand, since it provides simplifications for explicit choices of external helicity states. In other cases, one may instead make a list of all the loop-dependent objects (scalar products, spinor chains, etc. . .) appearing in the integrand and express them individually as functions of the variables y_j and μ_{ij} . This defines a list of substitutions which can instead be done numerically inside the linear fit procedure, through the definition of the auxiliary functions \mathbf{a} appearing in Eq. (4.10), while keeping the integrand written as a rational function of objects which yield a more compact expression for it.

As we explained, on a multiple cut, the variables y_j and μ_{ij} are no longer all independent, but a subset of them can be written as rational functions of the others. Once again, we note that one does not need to perform these substitutions explicitly in the integrand, but only numerically using the auxiliary functions \mathbf{a} as before.

We finally remark that it is often a good idea to group together diagrams which share the same denominator structure or can be put under the same set of denominators as one of the parent topologies of the process. Thanks to the fact that, in the linear fit algorithm we defined in Eq. (4.10), we allow an arbitrary sum of contributions on the r.h.s., this grouping can be easily performed by including each diagram in this list of contributions (which, we recall, here includes the integrand and the subtraction terms), without having to explicitly sum them up analytically.

8 Decomposition of amplitudes into form factors

In this section, we briefly discuss the possibility of using the FINITEFLOW framework for an alternative and widely used method for expressing amplitudes as linear combinations of standard Feynman integrals.

The method consists of considering an amplitude stripped of all the external polarization states. This amplitude will have a set of free indexes $\lambda_1 \dots, \lambda_e$, which may be Lorentz indexes, spinor indexes, or other indexes representing higher-spin states. One can thus write down the most general linear combination of tensors $T_j^{\lambda_1 \dots \lambda_e}$ having these indexes, compatible with the known properties of the amplitude, such as gauge invariance and other constraints. More explicitly

$$A^{\lambda_1 \dots \lambda_e} = \sum_j F_j T_j^{\lambda_1 \dots \lambda_e}. \quad (8.1)$$

The *form factors* F_j are rational functions of the kinematic invariants, which can be computed by contracting the amplitude on the l.h.s. with suitable projectors $P^{\lambda_1 \dots \lambda_e}$

$$F_j = P_j \cdot A, \quad (8.2)$$

where

$$P_j^{\lambda_1 \dots \lambda_e} = \sum_k T_{jk}^{-1} T_k^{\lambda_1 \dots \lambda_e} \quad (8.3)$$

with

$$T_{ij} \equiv T_i \cdot T_j. \quad (8.4)$$

In the previous equations, a dot product between two tensors is a short-hand for a full contraction between their indexes.

There are at least two bottlenecks in this approach for which the FINITEFLOW framework can be highly beneficial. The first is the inversion of the matrix defined in Eq. (8.4). This inversion can be obviously computed using one of the linear solvers described in section 4.2 – typically the dense solver if the tensors T_j do not have special properties of orthogonality. The inversion can also be performed numerically, since it is only required in an intermediate stage of the calculation, and can be represented by a node in the dataflow graph. We find that, even in cases where the inverse matrix is very complicated, its numerical inversion takes a negligible amount of time compared with other parts of the calculation (e.g. IBP reduction). The other bottleneck which can be significantly mitigated by our framework is the difficulty of computing the contraction on the r.h.s. of Eq. (8.2), in cases where the projectors are particularly complicated. Indeed, by substituting Eq. (8.3) into Eq. (8.2) we get

$$F_j = \sum_k T_{jk}^{-1} (T_k \cdot A). \quad (8.5)$$

This means that we can compute the contractions $T_k \cdot A$ instead, which are usually significantly simpler, and multiply them (numerically) by the matrix T_{jk}^{-1} at a later stage. This allows to reconstruct the form factors directly without ever needing explicit analytic expressions for the projectors. One can further elaborate the algorithm by contracting the free indexes of Eq. (8.1) with explicit polarization states, for the direct reconstruction of helicity amplitudes rather than the form factors themselves.

9 Finding integrable symbols from a known alphabet

As we already stated, many Feynman integrals can be cast as iterated integrals in the form of Eq. (6.5). It is customary to associate to these integrals an object called *symbol* [37, 51]. For the purposes of this paper, we define the symbol as

$$\mathcal{S} \left(\int d \log w_1 \circ d \log w_2 \circ \dots \right) \equiv w_1 \otimes w_2 \otimes \dots, \quad (9.1)$$

where, as already mentioned in section 6.2, w_k are called *letters*, and a complete set of letters $W = \{w_k\}$ is called *alphabet*. Because the symbol does not depend on the integration path and the boundary terms, it contains less information than the full iterated integral, but it is still a very interesting object to study for determining the analytic structure of an amplitude. More information on symbols, their properties, and their relations to multiple polylogarithms can be found in [51].

Given a known alphabet W , one can build symbols of *weight* n as linear combinations of those defined in Eq. (9.1), namely

$$S = \sum_{j_1, \dots, j_n} c_{j_1 \dots j_n} w_{j_1} \otimes \dots \otimes w_{j_n}. \quad (9.2)$$

However, in general, such a linear combination is not *integrable*, i.e. it does not integrate to a function which is independent of the integration path. As pointed out in [52], a necessary and sufficient condition for the symbol in Eq. (9.2) to be integrable is

$$\sum_{j_1, \dots, j_n} c_{j_1 \dots j_n} \left(\frac{\partial \log w_{j_k}}{\partial z_l} \frac{\partial \log w_{j_{k+1}}}{\partial z_m} - (l \leftrightarrow m) \right) w_{j_1} \otimes \dots \otimes \hat{w}_{j_k} \otimes \hat{w}_{j_{k+1}} \otimes \dots \otimes w_{j_n} = 0, \quad (9.3)$$

for all $k = 1, \dots, n - 1$ and all pairs (z_l, z_m) , where $\mathbf{z} = \{z_j\}$ are the kinematic variables the letters depend on. In the previous equation, \hat{w}_k indicates the omission of the letter w_k . By solving these integrability conditions, which amounts to solve a linear system for the coefficients $c_{j_1 \dots j_n}$, one can build a complete list of integrable symbols of weight n . It is worth mentioning that there are additional conditions one can impose to restrict the number of terms in the ansatz of Eq. (9.2), namely additional conditions on the allowed entries of a symbol. For instance, the first entry, which is related to the discontinuity of the function, may be restricted to contain only letters associated to physical branch points of an amplitude.

Here we discuss a simple method⁵ for finding all integrable symbols from a known alphabet, up to a specified weight n , exploiting the algorithms of the framework we presented in this paper.

We first observe that the only dependence of Eq. (9.3) on the explicit analytic expressions of the letters is via the crossed derivatives

$$d_{ij}^{(lm)} \equiv \frac{\partial \log w_i}{\partial z_l} \frac{\partial \log w_j}{\partial z_m} - (l \leftrightarrow m). \quad (9.4)$$

In order to simplify the notation, let us define a multi-index $J = (i, j, l, m)$ such that

$$d_J \equiv d_{ij}^{(lm)}. \quad (9.5)$$

The only relevant information about these derivatives which is needed for the purpose of solving Eq. (9.3) are possible linear relations which may exist between different elements d_J . These relations only depend on the alphabet, and not on the weight of the symbols which need to be considered. Once all these linear relations have been found for a given alphabet, the integrability conditions can be solved at any weight using a numeric linear system over \mathbb{Q} , and without using the analytic expressions of the letters again.

In order to find these linear relations, we first compute analytic expressions for all the functions d_J , which can usually be done in seconds even for complex alphabets. If the functions d_J have no square root in them, we simply solve the *linear-fit* problem

$$\sum_J x_J d_J = 0, \quad (9.6)$$

where the unknowns x_J are \mathbb{Q} -numbers, while the functions d_J depend on the variables \mathbf{z} . This equation is solved with respect to the unknowns x_J using the (numerical version of the) linear fit algorithm already described in this paper. Linear relations between the unknowns x_J are thus easily translated into relations between the functions d_J (notice that independent unknowns multiply dependent functions, and the other way around). In order to simplify the linear fit, it is convenient to extract a priori some obvious relations, such as relations of the form $d_J = 0$ or $d_{J_1} = \pm d_{J_2}$, which are more easily identifiable from the analytic expressions.

If the functions d_J depend on a set of (independent) square roots, we first rewrite each of them in a canonical form, such that each function is multi-linear in the square roots. This can be easily done, one square root at the time, by replacing a given square root \sqrt{f} with an auxiliary variable, say r , and computing the remainder of $d_J = d_J(r)$ with respect to $r^2 - f$, via a univariate polynomial division with respect to r (note that univariate polynomial

⁵This method has been independently developed by the author and used in several unpublished tests and checks (see e.g. ref. [53]). It shares some similarities with the one implemented in [54].

remainders are easily generalized to apply to rational functions⁶). The result will be linear in r . If all the square roots are chosen to be independent, after putting the functions d_J in this canonical form, one can simply solve the linear fit in Eq. (9.6) by replacing each square root with a new independent variable. This works because, if Eq. (9.6) holds and the d_J are put in this canonical form, then the terms multiplying independent monomials in the square roots must vanish separately. This is effectively equivalent to performing a linear fit where each square root is treated as an independent variable. We find that, even in cases where square roots are rationalizable, this approach is often more efficient than using a change of variables which rationalizes the square roots.

Once a complete set of linear relations between the crossed derivatives d_J has been found, one can use this information alone to solve the integrability conditions. This is best done recursively from lower to higher weights. As already stated, we understand that other conditions may still restrict the ansatz at any weight and therefore the list of integrable symbols.

At weight $n = 1$, every letter trivially defines an integrable symbol. At higher weights, it is customary to exploit the lower weight information in order to build a smaller ansatz than the one in Eq. (9.2). If $\{S_j^{(n-1)}\}_j$ is a complete set of integrable symbols at weight $n - 1$, we find the integrable symbols $S_j^{(n)}$ at weight n as follows. We write our ansatz as

$$S = \sum_{jk} c_{jk} S_j^{(n-1)} \otimes w_k. \quad (9.7)$$

Because the symbols $S_j^{(n-1)}$ are already integrable, we only need to impose the integrability condition on the last two entries. Hence, for all possible pairs of variables (z_l, z_m) we make the substitution

$$w_{j_1} \otimes \cdots \otimes w_{j_n} \rightarrow (w_{j_1} \otimes \cdots \otimes w_{j_{n-2}}) d_{j_{n-1}j_n}^{(lm)} \quad (9.8)$$

into Eq. (9.7), while $d_{j_{n-1}j_n}^{(lm)}$ are left as arbitrary variables (i.e. without explicitly substituting their expressions, which are no longer relevant at this stage). Then we substitute the linear relations satisfied by the $d_{j_{n-1}j_n}^{(lm)}$ such that our ansatz is written in terms of linearly independent functions (still represented by independent variables in the formulas), and we impose that the coefficient of each independent structure with the form of the r.h.s. of (9.8) vanishes. This strategy builds a numeric *sparse linear system* of equations for the coefficients c_{jk} in Eq. (9.7), which can be solved with the algorithm already discussed in this paper. Linear relations between the coefficients c_{jk} are then easily translated into a set of linearly independent symbols at weight n satisfying the integrability conditions.

10 Proof-of-concept implementation

With this paper, we also publicly release a proof-of-concept implementation of the FINITE-FLOW framework. The code is available here

<https://github.com/peraro/finiteflow>

and can be installed and used following the instructions given at that URL. This code is the result of experimentation and trial and error, and should not be regarded as an example of

⁶For instance, one can use the built-in MATHEMATICA procedure `PolynomialRemainder`, which applies to rational functions as well.

high coding standards or as a final implementation of this framework. Despite this, it has already been used for obtaining several cutting-edge research results in high energy physics, and we believe its public release can be highly beneficial to the community. It also includes the FINITEFLOW package for MATHEMATICA, which provides a high-level interface to the routines of the library.

We also release a collection of packages and examples using the MATHEMATICA interface to this code, at the URL

<https://github.com/peraro/finiteflow-mathtools>

which includes several applications described in this paper. In particular, it contains the following packages:

FFUtils Utilities implementing simple general purpose algorithms, such as algorithms for finding linear relations between functions.

LiteMomentum Utilities for momenta in Quantum Field Theory. It does not use FINITEFLOW, but it is used by other packages and examples in the same repository.

LiteIBP Utilities and tools for generating IBP systems of equations and differential equations for Feynman integrals, to be used together with the LITERED [31] package.

Symbols Scripts for building integrable symbols from known alphabets.

We note that these packages should be regarded as a set of utilities rather the implementation of fully automated solutions for specific tasks. They are also meant as examples of how to build packages on top of the MATHEMATICA interface to the code. The same repository also contains several examples of usage of the FINITEFLOW package. While these examples have been chosen to be simple enough to run in a few minutes on a modern laptop, they can be used as templates to be adapted to significantly more complex problems. We therefore recommend reading the documentation which comes with them and the comments inside their source as an introduction to the usage of this code for the applications described in this paper.

In this section, we give some details on some aspects and features of our implementation of the FINITEFLOW framework and provide some observations about possible improvements for the future.

The code is implemented in C++ and we provide a high-level MATHEMATICA interface. At the time of writing, the MATHEMATICA interface is the easiest and more flexible way of using FINITEFLOW, since it allows to combine the features of our framework with the ones of a full computer algebra system. Interfaces to other high-level languages, such as PYTHON, and computer algebra systems are likely to be added in the future.

This implementation uses finite fields \mathbb{Z}_p where p are 63-bit integers. We have explicitly hard-coded a list of primes satisfying $2^{63} > p > 2^{62}$ – namely the 201 largest primes with this property – which define all the finite fields we use. In particular, by making the assumption that all the primes we use belong to that range, we are able to perform a few optimizations in basic arithmetic operations. We use a few routines and macros of the FLINT library for basic operations of modular arithmetic (we also optionally provide a heavily stripped down version of FLINT with only the parts which are needed for FINITEFLOW, with fewer dependencies, as well as an easier and faster installation), such as the calculation of multiplicative inverses and modular multiplication using extended precision and precomputed reciprocals [55].

We use several representations of polynomials and rational functions, depending on the task. As already explained in section 4.1, if we need to repeatedly evaluate polynomials and rational functions, we store the data representing them as a contiguous array of integers and evaluate them by means of the Horner scheme. For polynomials in Newton’s representation, we store an array with the sequence $\{y_j\}$ and another one with the coefficients a_j . The latter is an array of integers in the univariate case (see Eq. (2.5)) and an array of Newton polynomials in fewer variables in the multivariate case (see Eq. (2.9)). Univariate rational functions in Thiele’s representation (given in Eq. (2.8)) are stored similarly to univariate Newton polynomials. For every other task, we use a sparse polynomial representation which consists of a list of non-vanishing monomials. Each monomial is, in turn, a numerical coefficient (in \mathbb{Z}_p or \mathbb{Q}) and an associated list of exponents for the variables. This representation is used for most algebraic operations on polynomials, e.g. when converting Newton’s polynomials in a canonical form, or when shifting variables (we recall that a shift of variables is typically required by the functional reconstruction algorithm we use). It is also the most convenient representation for communicating polynomial expressions between FINITEFLOW and other programs such as computer algebra systems.

Our system for dataflow graphs distinguishes several types of objects, namely *sessions*, *graphs*, *nodes* and *algorithms*.

Sessions are objects which contain a list of graphs and are responsible for doing most operations using them, such as evaluating them while handling parallelization, and running functional reconstruction algorithms. Since a session can contain any number of dataflow graphs, for most applications there is no reason for using more than one session in the same program, although it is obviously possible. The concept of a session is not (explicitly) present in the MATHEMATICA interface since the latter only uses one global session. Graphs in the same session, as well as nodes in a graph, are associated with a non-negative integer ID. In the MATHEMATICA interface, these IDs can instead be any expression, which is seamlessly mapped to the correct integer ID when communicating with the C++ code. Graphs, as already explained, are collections of nodes. Nodes are implemented as wrappers around algorithms and contain a list of IDs corresponding to their inputs. When building a new node for a graph, the program checks that the expected lengths of its input lists are consistent with the ones of the output lists of its input nodes. Algorithms are the lowest-level objects responsible for the numerical evaluations, and they have associated procedures for it. Algorithms might also have a procedure for their learning phase and, in that case, they also specify how many times this should be called (with different inputs).

Because an algorithm might have to run in parallel for different input values, it is made of two types of data. The first type is read-only data, i.e. data which is not specific to an evaluation point and can be shared across several threads during parallelization. This might also include data which is mutable only during the learning phase. The second type of data can instead be modified during any numerical evaluation. In multi-threaded applications, mutable data needs to be cloned across all the threads in order to avoid data races. Algorithm objects thus have associated routines for cloning mutable data.

In the future, we might further split mutable data into two types. The first is mutable data which only depends on the finite field \mathbb{Z}_p . This data only needs to be copied a number of times equal to the maximum number of fields used at the same time in a parallel evaluation, which is typically no larger than two. The second is data which can depend on both the prime p and the variables \mathbf{z} which are the input of a given graph. Only for the latter one needs to make a copy for each thread. Therefore, even though it is not currently implemented, this

further split can improve memory usage by significantly reducing the amount of cloned data. As an example, consider a linear system with parametric entries depending on variables \mathbf{z} . The rational functions defining the entries of the system as rational functions over \mathbb{Q} , as well as the list of independent unknowns and equations, are immutable data. The same functions mapped with over \mathbb{Z}_p depend on the prime p but not on the points \mathbf{z} . Finally, the numerical system, obtained by evaluating such functions numerically for specific inputs \mathbf{z} , depends on both the prime field and the evaluation point.

We point out that the usage of dataflow graphs also greatly simplifies multi-threading. It is indeed sufficient that each type of basic algorithm has an associated procedure for cloning its non-mutable data. From these, the framework is able to automatically clone the mutable data of any complex graph, and correctly use it for the purpose of performing multi-threaded evaluations. A similar potential advantage regards serialization of algorithms, although this feature is not implemented at the time of writing. In principle, each basic algorithm may have an associated procedure for serializing and deserializing its data. From these, one would be able to serialize complete graphs representing arbitrarily complex calculations. This could be useful for both sharing graphs and loading them up more quickly, together with the information about the learning phases which have already been completed.

We now turn to the caching system used to store the evaluations of a graph. We recall that, in the multivariate case, we start by performing some preliminary univariate reconstructions, which determine (among other things) a list of evaluation points needed to reconstruct the output of a graph. In principle, for each evaluation point, we may need to store the input variables, the whole output list of the graph, and the prime p which defines the finite field. Unfortunately, when the output of a graph is a long list and a large number of evaluation points is needed, this straightforward strategy can yield issues related to memory usage. This can be true even when a Non-Zeros node is appended to a graph (see section 4.4), as we have already recommended. Hence, we adopt a slightly more refined strategy which works well in realistic scenarios. Heuristically, we observe that, when the output of a graph is a long list, the complexity of the elements of the list can vary significantly. In particular, many elements correspond to relatively simple rational functions while, usually, only a few of them have high complexity. Simpler rational functions obviously need fewer evaluation points in order to be reconstructed. Hence, one could improve this strategy by storing a shorter output list containing, for each evaluation point, only the elements of the output which need that point for their reconstruction. In practice, we proceed as follows. Once a complete list of evaluation points has been determined, for each element of the output we tag all the points needed for its reconstruction. In our implementation, this tagging requires one bit of memory for each output element. If an evaluation point is never tagged, it is removed from the list. Then, after a graph is evaluated on a given point, we only store the entries of the output for which that point is needed. This typically allows to store a much shorter output list on most evaluation points, therefore yielding a major improvement in memory usage. When combined with Non-Zeros nodes, we find that with this strategy the caching of the evaluations is hardly ever a bottleneck in terms of memory usage, especially when the code is run on high-memory machines available in clusters and other computing facilities often used for intensive scientific computations.

We also point out that, as explained more in detail in section 10.1, one can generate lists of needed evaluation points and separately evaluate subsets of them, either sequentially or in parallel. On top of being a powerful option for parallelization, this feature also allows to split long calculations into smaller batches and save intermediate results to disk, such that they

are not lost in case of system crashes or other errors which may prevent the evaluations to successfully complete.

The FINITEFLOW library implements the basic numerical algorithms described in this paper, the functional reconstruction methods we discussed, as well as the framework based on dataflow graphs. When the latter is used, one can easily define complex numerical algorithms without any low-level coding. This can be done even more easily from the MATHEMATICA interface. The latter also offers some convenient wrappers for common tasks, such as solving analytic or numeric linear systems or linear fits. These wrappers hide the dataflow-based implementation. However, as discussed in this paper, the approach based on dataflow graphs offers a flexibility which greatly enhances the scope of possible applications of this framework.

The approach based on dataflow graphs is the preferred way of defining algorithms with the library, especially when using the MATHEMATICA interface. However, the library can also be enhanced by custom numerical algorithms written in C++. For instance, the results presented in [14, 42] used a custom C++ extension of the linear fit algorithm which computes generalized unitarity cuts via Berends-Giele currents, as explained in ref. [2] (this extension is not included in the public code).

It should also be clear that the FINITEFLOW framework is not designed to solve one specific problem, but as a method to implement solutions for a large variety of algebraic problems. By building on top of this public code, one can, of course, implement higher-level and easier-to-use solutions for more specific tasks.

10.1 Parallel execution

As discussed in section 2.3, one of the main advantages of functional reconstruction algorithms is that they can be massively parallelized. In our current implementation, we offer two strategies for parallelization, which can also be used together.

The first and easier-to-use strategy is *multi-threading*. This is handled completely automatically by the code when the dataflow-based approach is used. Data which cannot be shared among threads is cloned as needed and parallelization is achieved by splitting the calculation over an appropriate number of threads, as explained in section 2.3. The number of threads which is used can either be specified manually or chosen automatically based on the hardware configuration. We recommend specifying it manually when using the code on clusters or machines shared among several users, since the automatic choice might not be the most appropriate one in such cases.

The second method allows to further enhance parallelization possibilities by using several nodes of a cluster, or even several (possibly unrelated) machines, for the evaluations of the function to be reconstructed. In order to use this method, after defining a numerical algorithm, we compute and store the total and partial degrees of its output. As explained, this is done via univariate reconstructions which are much quicker than a full multivariate one. From this information, we also build and store a list of inputs for the evaluations. For this, we need to make a guess of how many prime fields will be needed. One can, however, start by assuming only one prime field is needed, and add more points at a later time if this is not the case. The stored list of needed evaluation points can be shared across several nodes or several machines, where any subset of them can be computed and saved independently. Of course, these evaluations can (and will, by default) be further parallelized using multi-threading, as discussed above. Finally, the evaluations are collected on one machine where the reconstruction is performed. Should the reconstruction fail due to the need of more prime

fields, we increase our guess on the number of primes needed and create a complementary list of evaluation points. We then proceed with the evaluation of these additional points, across several nodes or machines as for the previous one, and collect them for the reconstruction. We proceed this way until the reconstruction is successful. This method greatly increases the potential parallelization options, at the price of being less automated, since the lists of evaluations need to be generated and copied around by hand.⁷ This option can be very beneficial for reconstructing particularly complex functions, or functions whose numerical evaluation is very time-consuming. As already mentioned, it also provides a method splitting up long calculations in smaller batches and saving intermediate results on disk.

11 Conclusions

We presented the FINITEFLOW framework, which establishes a novel and effective way of defining and implementing complex algebraic calculations. The framework comprises an efficient low-level implementation of basic numerical algorithms over finite fields, a system for easily combining these basic algorithms into computational graphs – known as dataflow graphs – representing arbitrarily complex algorithms, and multivariate functional reconstruction techniques for obtaining analytic results of out these numerical evaluations.

Within this framework, complex calculations can be easily implemented using high-level languages and computer algebra systems, without being concerned with the low-level details of the implementation. It also offers a highly automated way of parallelizing the calculation, thus fully exploiting available computing resources.

The framework is easy to use, efficient, and extremely flexible. It can be employed for the solution of a huge variety of algebraic problems, in several fields. It allows to directly reconstruct analytic expressions for the final results of algebraic calculations, thus sidestepping the appearance of large intermediate expressions, which are typically a major bottleneck.

In this paper, we have shown several applications of this framework to highly relevant problems in high-energy physics, in particular concerning the calculation of multi-loop scattering amplitude.

We also release a proof-of-concept implementation of this framework. This implementation has already been successfully applied to several state-of-the-art problems, some of which proved to be beyond the reach of traditional computer algebra, using reasonable computing resources. Notable examples are recent results for two-loop five-gluon helicity amplitudes in Yang-Mills theory [14,21] and the reduction of four-loop form factors to master integrals [17]. We point out that these two types of examples are complex for very different reasons. In the former, a large part of the complexity is due to the high number of scales, while in the latter, which only has one scale, it is due to the huge size of the IBP systems one needs to solve. Quite remarkably, the techniques described in this paper have been able to tackle both these cases, showing that they are capable of dealing with a wide spectrum of complex problems.

We believe the algorithms presented in this paper, and their publicly released proof-of-concept implementation, will contribute to pushing the limits of what is possible in terms of algebraic calculations. Due to their efficiency and flexibility, they will be useful in the future

⁷ In the future, we might consider implementing other approaches, such as the use of the standard MESSAGE PASSING INTERFACE (MPI) to offer a more automated way of parallelizing the evaluations across several nodes of the same cluster. However, the latter approach would end up being more limiting than the one we already implemented, since MPI does not support parallelization over several unrelated machines.

for obtaining more scientific results concerning a wide range of problems.

Acknowledgements

I thank Simon Badger, Johannes Henn, Pierpaolo Mastrolia, and Lorenzo Tancredi for many discussions, comments, and for their collaboration on topics which motivated the development of the methods presented in this paper. I am also grateful to Simon Badger, Christian Brønnum-Hansen, Heribertus Bayu Hartanto, and William Torres Bobadilla for testing various features of the proof-of-concept implementation of these methods and providing valuable feedback. This project has received funding from the European Union’s Horizon 2020 research and innovation programme under the Marie Skłodowska-Curie grant agreement 746223.

Appendix A Mutability of graphs and nodes

In this appendix we discuss a technical aspect of our implementation of dataflow graphs, namely the *mutability* of graphs and nodes. In general, mutating nodes or graphs which have already been defined can lead to inconsistencies between the implemented algorithms and their expected inputs. However, depending on the use case, it may be convenient to have the ability of performing such mutations, to the extent that the defined graphs are always consistent.

Let us first discuss the mutability of *nodes*. Mutating a node can mean either deleting it, replacing it, or modifying its metadata in a way that changes its output (e.g. changing the list of needed unknowns in a linear system). We find it is convenient to allow such mutations, as long as a node is not used as input in any other node of a graph. Once a node N_1 is specified as input of another node N_2 , the input node N_1 becomes *immutable*, i.e. the mutations described above are no longer allowed. This is done in order to prevent changes of the length of the output of node N_1 which can make the evaluation of node N_2 impossible (note that in principle we may allow swapping two nodes which have the same lengths for the input and output lists, but this is currently not implemented). As a convenience, we allow to make node N_1 mutable again, after node N_2 and all other nodes using N_1 as input have been deleted.

We now turn to the mutability of *graphs*. In particular, this is relevant when using *subgraph* nodes. Mutating a graph may involve adding, deleting, or mutating its nodes, and changing its output node. Once a graph G_1 is specified as subgraph of a node N in another graph G_2 , then the graph G_1 becomes immutable. If this was not the case, mutations to the graph G_1 may modify its output and make node N , and therefore graph G_2 , impossible to evaluate. For the same reason, the output node of G_1 is also made immutable in such cases. Once all the nodes using G_1 as subgraph are deleted, graph G_1 becomes mutable again.

Appendix B Further observations on IBP identities

In this appendix we collect some observations about IBP identities which complement the discussion in section 5.1.

We already observed that, in order to solve any linear system, we must sort the unknowns by weight. Whenever we solve an equation, higher weight unknowns are expressed in terms of lower weight unknowns. The complexity of the Gauss elimination algorithm for a sparse

system can strongly depend on this choice of weight. Therefore, even if any choice of weight can be specified when defining a system, it is worth giving an example which we found works well for IBP systems.

In the case of an IBP system, the unknowns are Feynman integrals. For the purpose of assigning a weight to them, it is customary to associate to each integral in Eq. (5.1) the following numbers:

- t is the number of exponents α_j such that $\alpha_j > 0$
- r is the sum of the positive exponents

$$r = \sum_{j|\alpha_j>0} \alpha_j \tag{B.1}$$

- s is minus the sum of the negative exponents

$$s = - \sum_{j|\alpha_j<0} \alpha_j \geq 0. \tag{B.2}$$

It is generally understood that the higher these numbers are, the more complex an integral should be considered [30]. It is also customary to use the notion of *sector* of an integral, which is identified by the list of indexes j such that the exponents α_j are positive, i.e. $\{j|\alpha_j > 0\}$. In other words, two integrals belonging to the same sector depend on the same list of denominators, possibly raised to different powers, and possibly with a different numerator. As an example, a definition of weight for Feynman integral can be determined, by the following criteria, in order of importance:

- the positive integer $r - t$, where a higher number means higher weight
- the positive integer t , where a higher number means higher weight
- the positive integer r , where a higher number means higher weight
- the positive integer s , where a higher number means higher weight
- integrals in a topology T_1 are considered to be of higher weight if they belong to a sector mapped to a different topology T_2
- integrals in a sector of a topology T are considered to be of higher weight if they belong to a sector mapped to another sector of the same topology
- the positive integer $\max(\{-\alpha_j\}_{j|\alpha_j<0})$, where a higher integer means higher weight.

If the criteria above are not sufficient to uniquely sort two different integrals, we fall back to any other criterion which defines a total ordering, such as the intrinsic ordering built in a computer algebra system to sort expressions. The choice above prefers integrals with powers of denominators no higher than one – indeed, this is used as the very first criterion for determining the weight of a Feynman integrals. We found that this choice is particularly effective when combined with the mark-and-sweep algorithm for filtering out unneeded equations, since it often yields a smaller set of needed equations than other choices. We however stress again

that, of course, many other definitions of weight are possible and can be specified instead of the one suggested here.

We make a few more observations about the generation of IBP systems. These equations – which include IBPs, Lorentz invariance identities, symmetries among integrals of the same sectors, and mappings between integrals of different sectors – are typically first generated for generic Feynman integrals of the form of Eq. (5.1) with arbitrary symbolic exponents. These are sometimes called *template equations*. The IBP system is thus generated by writing down these template equations for specific Feynman integrals (i.e. for specific values of the exponents), which in this context are known as *seed integrals*. It is interesting to understand how many and which seed integrals must be chosen in order to successfully reduce a given set of needed integrals to master integrals. To the best of our knowledge, there is no way of determining a priori a minimal choice which works, but common choices which are expected to work in most cases (despite not being minimal) exist. A popular choice which usually works is selecting a range for the integers s and r of the seed integrals, based on the choice one must make for the top-level sectors. However, we find that it is often more convenient to specify a range in s and $r - t$ instead. In particular, for most topologies one only needs to select seed integrals for which the value of $r - t$ is either the same or one unity higher than the maximal one between the integrals which need to be reduced. We however also point out that, while an over-conservative choice of seed integrals will result in a slowdown of the learning phase, the equations generated from unneeded seed integrals may be all successfully filtered out by the mark-and-sweep algorithm, hence reducing the system to the same one would have obtained with a more optimal choice. However, we also point out that this may or may not happen depending on the chosen ordering for the Feynman integrals. We have empirically observed that it does happen for the choice of ordering based on the definition of weight we suggested above.

We conclude this appendix with an observation about sector mappings which we haven't found elsewhere in the literature. This concerns kinematic configurations which have symmetries with respect to permutations of external legs, i.e. permutations of external momenta which preserve all the kinematic invariants. Notable examples are three-point kinematics with two massless legs, and four-point fully massless kinematics. For these kinematic configurations we can distinguish two types of sector mappings. The first one, which we call here *normal mappings*, simply consists of shifts of the loop momenta which map a sector into a different one. The second one, which we call *generalized mappings*, consists of a permutation of external legs which preserves the kinematic invariants, optionally followed by a shift of the loop momenta. The most typical approach to deal with these mappings does not distinguish between the two types. In particular, for all mapped sectors, only sector mappings are generated in the system of equations, and no IBP identity, Lorentz identity or sector symmetry. The rationale is that one would expect the other identities to be automatically covered by combining sector mappings with identities generated for the unique (unmapped) sectors. However, we explicitly verified that this is not always the case for generalized mappings. In other words, given a set of seed integrals for a generalized mapped sector, there are some identities which are independent of the ones generated by combining sector mappings for the same set of seed integrals, and identities for the unique sectors. The missing identities can be recovered by adding more seed integrals to the mapped sectors and to the unique sectors, at the price of obtaining a more complex system of equations. Notice that this is similar to what happens for Lorentz invariance identities, which in principle can be replaced by IBP identities only, at the price of using more seed integrals and making the system more complex. A simple

example of this is the two-loop massless double box. We indeed found that this topology can be reduced to master integrals, for any range in s , by considering only seed integrals with $r - t = 0$, as long as IBPs and Lorentz invariance identities are generated also for sectors satisfying generalized mappings. When these additional identities are not included, we need to add seed integrals with $r - t = 1$ in order to successfully perform the reduction. We therefore recommend to generate, alongside generalized mappings, also IBPs, Lorentz identities and symmetries for sectors which satisfy them. This is even more convenient when using the mark-and-sweep algorithm for simplifying the system, since the simpler equations with lower $r - t$ are automatically selected if available. This can eventually yield a smaller system with easier equations to solve. For similar reasons, we recommend to always add Lorentz invariance identities, regardless of the topology.

References

- [1] A. von Manteuffel and R. M. Schabinger, *A novel approach to integration by parts reduction*, *Phys. Lett.* **B744** (2015) 101–104, [[1406.4513](#)].
- [2] T. Peraro, *Scattering amplitudes over finite fields and multivariate functional reconstruction*, *JHEP* **12** (2016) 030, [[1608.01902](#)].
- [3] G. Ossola, C. G. Papadopoulos, and R. Pittau, *Reducing full one-loop amplitudes to scalar integrals at the integrand level*, *Nucl. Phys.* **B763** (2007) 147–169, [[hep-ph/0609007](#)].
- [4] W. T. Giele, Z. Kunszt, and K. Melnikov, *Full one-loop amplitudes from tree amplitudes*, *JHEP* **04** (2008) 049, [[0801.2237](#)].
- [5] P. Mastrolia and G. Ossola, *On the Integrand-Reduction Method for Two-Loop Scattering Amplitudes*, *JHEP* **11** (2011) 014, [[1107.6041](#)].
- [6] S. Badger, H. Frellesvig, and Y. Zhang, *Hepta-Cuts of Two-Loop Scattering Amplitudes*, *JHEP* **04** (2012) 055, [[1202.2019](#)].
- [7] Y. Zhang, *Integrand-Level Reduction of Loop Amplitudes by Computational Algebraic Geometry Methods*, *JHEP* **09** (2012) 042, [[1205.5707](#)].
- [8] P. Mastrolia, E. Mirabella, G. Ossola, and T. Peraro, *Scattering Amplitudes from Multivariate Polynomial Division*, *Phys. Lett.* **B718** (2012) 173–177, [[1205.7087](#)].
- [9] Z. Bern, L. J. Dixon, D. C. Dunbar, and D. A. Kosower, *One loop n point gauge theory amplitudes, unitarity and collinear limits*, *Nucl. Phys.* **B425** (1994) 217–260, [[hep-ph/9403226](#)].
- [10] Z. Bern, L. J. Dixon, D. C. Dunbar, and D. A. Kosower, *Fusing gauge theory tree amplitudes into loop amplitudes*, *Nucl. Phys.* **B435** (1995) 59–101, [[hep-ph/9409265](#)].
- [11] R. Britto, F. Cachazo, and B. Feng, *Generalized unitarity and one-loop amplitudes in $N=4$ super-Yang-Mills*, *Nucl. Phys.* **B725** (2005) 275–305, [[hep-th/0412103](#)].
- [12] R. K. Ellis, W. T. Giele, and Z. Kunszt, *A Numerical Unitarity Formalism for Evaluating One-Loop Amplitudes*, *JHEP* **03** (2008) 003, [[0708.2398](#)].

- [13] A. von Manteuffel and R. M. Schabinger, *Quark and gluon form factors to four-loop order in QCD: the N_f^3 contributions*, *Phys. Rev.* **D95** (2017), no. 3 034030, [[1611.00795](#)].
- [14] S. Badger, C. Brønnum-Hansen, H. B. Hartanto, and T. Peraro, *Analytic helicity amplitudes for two-loop five-gluon scattering: the single-minus case*, *JHEP* **01** (2019) 186, [[1811.11699](#)].
- [15] S. Abreu, J. Dormans, F. Febres Cordero, H. Ita, and B. Page, *Analytic Form of the Planar Two-Loop Five-Gluon Scattering Amplitudes in QCD*, *Phys. Rev. Lett.* **122** (2019), no. 8 082002, [[1812.04586](#)].
- [16] R. N. Lee, A. V. Smirnov, V. A. Smirnov, and M. Steinhauser, *Four-loop quark form factor with quartic fundamental colour factor*, *JHEP* **02** (2019) 172, [[1901.02898](#)].
- [17] J. M. Henn, T. Peraro, M. Stahlhofen, and P. Wasser, *Matter dependence of the four-loop cusp anomalous dimension*, [1901.03693](#).
- [18] A. von Manteuffel and R. M. Schabinger, *Quark and gluon form factors in four loop QCD: the N_f^2 and $N_{q\gamma}N_f$ contributions*, [1902.08208](#).
- [19] S. Abreu, J. Dormans, F. Febres Cordero, H. Ita, B. Page, and V. Sotnikov, *Analytic Form of the Planar Two-Loop Five-Parton Scattering Amplitudes in QCD*, [1904.00945](#).
- [20] A. Von Manteuffel and R. M. Schabinger, *Planar master integrals for four-loop form factors*, [1903.06171](#).
- [21] S. Badger, D. Chicherin, T. Gehrmann, G. Heinrich, J. M. Henn, T. Peraro, P. Wasser, Y. Zhang, and S. Zoia, *Analytic form of the full two-loop five-gluon all-plus helicity amplitude*, [1905.03733](#).
- [22] J. Klappert and F. Lange, *Reconstructing Rational Functions with FireFly*, [1904.00009](#).
- [23] M. Abadi, A. Agarwal, P. Barham, E. Brevdo, Z. Chen, C. Citro, G. S. Corrado, A. Davis, J. Dean, M. Devin, S. Ghemawat, I. Goodfellow, A. Harp, G. Irving, M. Isard, Y. Jia, R. Jozefowicz, L. Kaiser, M. Kudlur, J. Levenberg, D. Mané, R. Monga, S. Moore, D. Murray, C. Olah, M. Schuster, J. Shlens, B. Steiner, I. Sutskever, K. Talwar, P. Tucker, V. Vanhoucke, V. Vasudevan, F. Viégas, O. Vinyals, P. Warden, M. Wattenberg, M. Wicke, Y. Yu, and X. Zheng, *TensorFlow: Large-scale machine learning on heterogeneous systems*, 2015. Software available from tensorflow.org.
- [24] P. S. Wang, *A p -adic algorithm for univariate partial fractions*, in *Proceedings of the Fourth ACM Symposium on Symbolic and Algebraic Computation*, SYMSAC '81, (New York, NY, USA), pp. 212–217, ACM, 1981.
- [25] P. S. Wang, M. J. T. Guy, and J. H. Davenport, *P -adic reconstruction of rational numbers*, *SIGSAM Bull.* **16** (May, 1982) 2–3.
- [26] M. Abramowitz and I. Stegun, *Handbook of Mathematical Functions: With Formulas, Graphs, and Mathematical Tables*. Dover Publications, 1964.

- [27] A. Cuyt and W. shin Lee, *Sparse interpolation of multivariate rational functions*, *Theoretical Computer Science* **412** (2011), no. 16 1445 – 1456. Symbolic and Numerical Algorithms.
- [28] P. Maierhöfer, J. Usovitsch, and P. Uwer, *Kira—A Feynman integral reduction program*, *Comput. Phys. Commun.* **230** (2018) 99–112, [[1705.05610](#)].
- [29] P. Mastrolia, T. Peraro, and A. Primo, *Adaptive Integrand Decomposition in parallel and orthogonal space*, *JHEP* **08** (2016) 164, [[1605.03157](#)].
- [30] S. Laporta, *High precision calculation of multiloop Feynman integrals by difference equations*, *Int. J. Mod. Phys. A* **15** (2000) 5087–5159, [[hep-ph/0102033](#)].
- [31] R. N. Lee, *Presenting LiteRed: a tool for the Loop InTEgrals REDuction*, [1212.2685](#).
- [32] J. M. Henn, *Multiloop integrals in dimensional regularization made simple*, *Phys. Rev. Lett.* **110** (2013) 251601, [[1304.1806](#)].
- [33] A. V. Kotikov, *Differential equations method: New technique for massive Feynman diagrams calculation*, *Phys. Lett.* **B254** (1991) 158–164.
- [34] T. Gehrmann and E. Remiddi, *Differential equations for two loop four point functions*, *Nucl. Phys.* **B580** (2000) 485–518, [[hep-ph/9912329](#)].
- [35] P. Wasser, *Analytic properties of Feynman integrals for scattering amplitudes*, M.Sc. (2016) [<https://publications.ub.uni-mainz.de/theses/frontdoor.php?sourceopus=100001967>].
- [36] D. Chicherin, T. Gehrmann, J. M. Henn, P. Wasser, Y. Zhang, and S. Zoia, *All master integrals for three-jet production at NNLO*, [1812.11160](#).
- [37] A. B. Goncharov, M. Spradlin, C. Vergu, and A. Volovich, *Classical Polylogarithms for Amplitudes and Wilson Loops*, *Phys. Rev. Lett.* **105** (2010) 151605, [[1006.5703](#)].
- [38] S. Abreu, B. Page, and M. Zeng, *Differential equations from unitarity cuts: nonplanar hexa-box integrals*, *JHEP* **01** (2019) 006, [[1807.11522](#)].
- [39] G. 't Hooft and M. J. G. Veltman, *Regularization and Renormalization of Gauge Fields*, *Nucl. Phys.* **B44** (1972) 189–213.
- [40] Z. Bern, A. De Freitas, L. J. Dixon, and H. L. Wong, *Supersymmetric regularization, two loop QCD amplitudes and coupling shifts*, *Phys. Rev.* **D66** (2002) 085002, [[hep-ph/0202271](#)].
- [41] S. Abreu, F. Febres Cordero, H. Ita, M. Jaquier, and B. Page, *Subleading Poles in the Numerical Unitarity Method at Two Loops*, *Phys. Rev.* **D95** (2017), no. 9 096011, [[1703.05255](#)].
- [42] S. Badger, C. Brønnum-Hansen, H. B. Hartanto, and T. Peraro, *First look at two-loop five-gluon scattering in QCD*, *Phys. Rev. Lett.* **120** (2018), no. 9 092001, [[1712.02229](#)].
- [43] F. A. Berends and W. T. Giele, *Recursive Calculations for Processes with n Gluons*, *Nucl. Phys.* **B306** (1988) 759–808.

- [44] J. Gluza, K. Kajda, and D. A. Kosower, *Towards a Basis for Planar Two-Loop Integrals*, *Phys. Rev.* **D83** (2011) 045012, [[1009.0472](#)].
- [45] H. Ita, *Two-loop Integrand Decomposition into Master Integrals and Surface Terms*, *Phys. Rev.* **D94** (2016), no. 11 116015, [[1510.05626](#)].
- [46] K. J. Larsen and Y. Zhang, *Integration-by-parts reductions from unitarity cuts and algebraic geometry*, *Phys. Rev.* **D93** (2016), no. 4 041701, [[1511.01071](#)].
- [47] S. Abreu, F. Febres Cordero, H. Ita, B. Page, and M. Zeng, *Planar Two-Loop Five-Gluon Amplitudes from Numerical Unitarity*, *Phys. Rev.* **D97** (2018), no. 11 116014, [[1712.03946](#)].
- [48] A. Hodges, *Eliminating spurious poles from gauge-theoretic amplitudes*, *JHEP* **05** (2013) 135, [[0905.1473](#)].
- [49] S. Badger, H. Frellesvig, and Y. Zhang, *A Two-Loop Five-Gluon Helicity Amplitude in QCD*, *JHEP* **12** (2013) 045, [[1310.1051](#)].
- [50] S. Badger, *Automating QCD amplitudes with on-shell methods*, *J. Phys. Conf. Ser.* **762** (2016), no. 1 012057, [[1605.02172](#)].
- [51] C. Duhr, H. Gangl, and J. R. Rhodes, *From polygons and symbols to polylogarithmic functions*, *JHEP* **10** (2012) 075, [[1110.0458](#)].
- [52] F. C. S. Brown, *Multiple zeta values and periods of moduli spaces $M_{0,n}(\mathbb{R})$* , *Annales Sci. Ecole Norm. Sup.* **42** (2009) 371, [[math/0606419](#)].
- [53] **In** Collaboration, S. Zoia, *Conformal Symmetry and Feynman Integrals*, *PoS LL2018* (2018) 037, [[1807.06020](#)].
- [54] V. Mitev and Y. Zhang, *SymBuild: a package for the computation of integrable symbols in scattering amplitudes*, [1809.05101](#).
- [55] T. Granlund and N. Möller, *Improved division by invariant integers*, *IEEE Transactions on Computers* **60** (06, 2010) 165–175.